Mass spectrometry based method development for monitoring degradation of coffee beans and mechanistic exploration into methylation enhancement of phospholipids using diazomethane

by

John McFarlan

A thesis submitted to the Faculty of Graduate and Post Doctoral Affairs in partial fulfillment of the requirements for the degree of

Master of Science

in

Chemistry

Carleton University
Department of Chemistry
Ottawa, Ontario

Abstract

Mass spectrometry is a powerful analytical tool with endless potential for developing new scientific methods and making new discoveries in science.

In part I of this work, headspace GCMS was used to monitor and identify volatile chemicals, attributing to the unique flavours in roasted coffee, which diminished as the coffee beans aged. These flavour components were shown to vary in relative abundance randomly over time and the extent to which they varied was seemingly random as well. Though strong conclusions could not be made, comparing the change in peak area over a period of months appears to be an optimistic method to use in order to evaluate the coffee's quality with measurable accuracy.

In part II of this work, nanoESI mass spectrometry was used to show mechanistically how diazomethane methylates phospholipids. The methylation of sphingomyelin and phosphatidylethanolamine were shown to undergo complete conversion in different solvent mixtures.

Acknowledgements

I would like to thank my supervisor, Jeff Smith, for giving me the opportunity to work in his lab. You gave me so much freedom and support that it really allowed me to think clearly about my research and exercise my creativity. I am truly grateful for the skills and knowledge that I gained from this experience and through your professional resources; I am walking out of university and into my first job. You've been a great mentor throughout and I wish you all the best in years to come.

I would like to thank Karl Wasslen for all his help and expertise in the Carleton Mass Spectrometry Centre. Thank you for maintaining all the instruments and assisting me with my analyses whenever I needed help.

I would like to thank Ian Clark and Cliff Hansen of Bridgehead for their collaboration. I learned so much about coffee and really enjoyed working with you guys.

Lastly, I would like to thank my fiancé, Tracy, for all her love and support. You always inspire me and keep me motivated with everything I do. I owe much of my success to the support that you've given me. I am forever grateful to have met you and I can't wait to be with you for the rest of our lives.

Table of Contents

List of figures

List of tables

List of abbreviations

BeO – Berylium oxide

CsSb – Cesium/antimony alloy

Ether – Diethyl ether

EtOH – Ethanol

GaP – Gallium/phosphorus alloy

GCMS – Gas chromatography mass spectrometry

HBF_4 – Tetrafluoroboric acid

KOH (aq) – Aqueous potassium hydroxide

MeOH – Methanol

msms – Product ion scan

m/z – Mass to charge ratio

nanoESI – nano-electrospray ionization

NIST – National Institute of Standards and Technology

PC – Phosphatidylcholine

PE – Phosphatidylethanolamine

PEEK – Polyether ether ketone

pKa – ($-\log_{10}$) of the acid dissociation constant, Ka

SM – Sphingomyelin

Part I – Mass spectrometry based method development for monitoring degradation of coffee beans

Introduction

Gas Chromatography

1.1 History

Chromatography was discovered in 1903 by a Russian-Italian botanist named Mikhail Tsvet. Using calcium carbonate as the stationary phase, he separated chlorophylls and carotenoids in plant pigments using an organic solvent mixture of ethanol and ether as eluent.[1] This early discovery of chromatographic separation was eventually accepted amongst scientists and fuelled the development of liquid-liquid and paper chromatography by Archer John Porter, for which he shared the 1952 Nobel Prize in Chemistry.[2] Martin also developed the technique of gas-liquid chromatography in the early 1950s, which quickly lead to development of the gas chromatograph. In 1955, PerkinElmer introduced the Model 154 Vapor Fractometer, which was their first gas chromatograph that adjusted column temperature in an oven and used syringe injection and a flash vaporizer.[3]

1.2 How it works

1.2.1 Principles of headspace vial preparation

When analyzing dilute samples in solution, it is important to consider the concentration and the volume of solution being added to the headspace vial, as well as the vial equilibration time and temperature. Considering these factors is necessary for

increasing the concentration of sample in the headspace and thereby increasing the sensitivity of the analysis.

The volume of the sample solution is generally not more than half the volume of the vial. Larger volumes will increase the concentration of solvent in the headspace, which decreases sensitivity. This sensitivity loss would only be detrimental if the analyte concentration was too low for adequate detection.

The concentration of the analyte in the headspace can be increased by raising the vial equilibration temperature, equilibration time, and by adding salt to the sample solution. Increasing the vial equilibration temperature will increase the vapour pressure of the sample and a longer vial equilibration time will assure that the sample reaches equilibrium, which increases reproducibility. It is important to equilibrate the sample at a high enough temperature to increase the headspace concentration, while not exceeding the pressure limit of the vial.[4] Another method implemented to drive the analyte into the headspace is to add salt to the solution. Saturating an aqueous solution with salt shifts the liquid/gas equilibrium almost entirely to the gas phase due to the increased density of the solution. As a result, the analyte loses affinity to the solvent and its volatility increases. This increases the concentration of analyte in the headspace and increases sensitivity.

Dry samples also work well in headspace analysis. All the same concepts that apply to solution analysis apply to dry sample analysis, except the salting technique. The main difference in the two media is the nature of the headspace/sample equilibrium. While the solution solvates the analyte, the analyte adsorbs and desorbs from the dry sample matrix. Increasing the surface area of the dry sample by grinding it into a powder reduces the equilibration time since the analyte will be volatilized more readily.[4]

1.2.2 Headspace sampling

The headspace vials are partially filled with sample, capped and sealed with a crimper that forces the aluminum cap edge to form a seal tightly around the neck of the vial. The vials sit in a 12-vial auto-sampler station and are transferred sequentially and individually into the oven to equilibrate at a specified temperature for a specified amount of time. During the equilibration time, the sample in the vial is heating up and the low boiling components enter the headspace above the sample.

Once the heated sample has equilibrated, releasing as many volatile components as possible into the headspace, the sample is then ready to be injected into the transfer line. A needle pierces the septum of the vial cap and pressurizes the vial with nitrogen. Pressurizing the sample vial makes it much easier to withdraw from the headspace by not creating a vacuum within the vial. After pressurizing the sample vial with nitrogen, the headspace is withdrawn and injected into a heated loop, where it is mixed with

helium carrier gas and carried into the transfer line. The transfer line is usually 10°C warmer than the equilibration temperature to assure the volatile compounds reach the column, while minimizing adsorption to the transfer line.

1.2.3 Columns

Columns used in gas chromatography are designed in a variety of ways so that separation requirements of many different organic mixtures can be met by using the column best suited for the job.

Packed columns are made of glass or stainless steel, making them strong enough to withstand higher pressures than fused silica capillary columns. Their durability enables higher sample capacity, but packed columns are becoming obsolete because newly developed detectors require much less sample to achieve high sensitivity.[5]

Capillary columns are made of fused silica because it is a highly inert material that can support a wide variety of stationary phases. The two main types of capillary columns are wall coated open tubular (WCOT) and porous layer open tubular (PLOT) columns.[5] Wall coated capillary columns consist of a liquid film coating and the porous layer stationary phase is a solid material coating.[5] PLOT type columns are typically only used for resolving certain alkane isomers; otherwise the WCOT type columns are the most often used.[5]

1.2.4 Dynode cone detector

In GC-MS, as the ions leave the quadrupole mass analyzer, they collide with a mesh coated with electron-emitting material such as CsSb, GaP, or BeO.[6] The emitted electrons proceed into a dynode cone where the walls are coated with more electron-emitting material. As the electrons collide with the dynode surface, the electrons multiply exponentially, forming a cascade. The amplification can be on the order of 10^6 electrons, resulting in an output current, which is converted into a signal.[6]

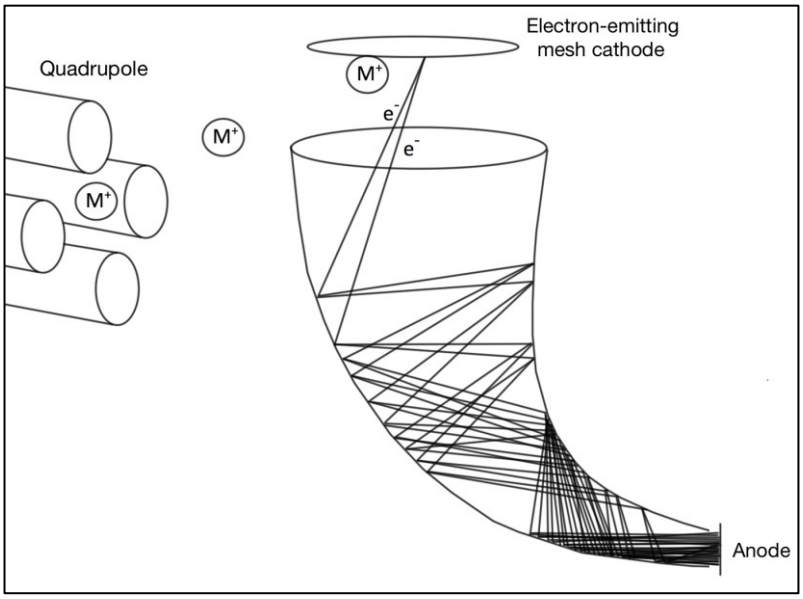

Figure 1.1: Dynode cone electron multiplier detector.

1.3 Why headspace GC-MS is the best

There are many reasons why headspace gas chromatography coupled with electron ionization mass spectrometry is ideal for coffee flavour analysis. Headspace is advantageous because only the low boiling components are injected, and so the analyte's relatively high vapour pressures eliminate residues, which keeps the column clean. Headspace injection also results in the most accurate representation of flavour composition because the injection contains a thermally equilibrated mixture of volatile compounds in their relative abundances.[7]

Electron ionization coupled with gas chromatography not only separates complex mixtures, but also produces multiple mass spectra within separated peaks. The ionization conditions are also standardized globally to 70 eV, which allows chemical spectra to be obtained and shared around the world in databases. The databases can then be used to compare and identify the species in the analyzed mixture. This dramatically simplifies the analysis of all complex mixtures, making GC-MS extremely advantageous for coffee analysis.

One disadvantage of headspace occurs when the analyte mixture is injected into the carrier gas over time instead of directly onto the column, resulting in peak broadening. Longer injection time and greater injection volume are the two contributing factors to broader peaks. This can be overcome by optimizing the injection conditions or

alternatively by cryofocusing the sample at the head of the column.[7] In 1990, Shimoda and Shibamoto found that by submerging a small portion of the column at the head in liquid nitrogen, the sample condensed and as the components separated on the column, they observed sharp, narrow and well-resolved peaks.[7]

Materials and methods

2.1 Sample roasting procedure

A sample of coffee (roughly 80-90 g) was dropped into the roasting drum at 350°F. The airflow valve was opened 75% and held in that position for 4.25 minutes. The airflow was then reduced to 25% and the roasting personnel awaited a “pop” or “crack” sound as a result of the beans releasing water vapour and carbon dioxide. Once the beans cracked, they were roasted for an additional 45 seconds. The coffee beans were then removed from the drum and cooled to room temperature in the cooling tray. Sample roasting was performed using a PROBAT 200 g capacity coffee sample roaster.

2.2 Coffee sample preparation

A Baratza Virtuoso grinder was set to 10 (out of 40) and the roasted coffee sample was coarsely ground. Approximately 1.1 g of ground coffee was weighed and added to a headspace vial. The headspace vial was topped with an aluminum cap and locked with an airtight seal using a crimping tool. The headspace vial was capped as quickly as possible to minimize loss of any volatile gases.

The headspace vials, caps, DB-WAXetr column, and the crimping tool were all purchased from Agilent.

2.3 Headspace-GCMS programs

Table 2.1: GC temperature program used for MeOH blanks.

	Temperature	Hold Time	Ramp Rate
Initial, T_1	50°C	2.00 min	10°C/min
T_2	120°C	0.00 min	20°C/min
T_3	235°C	5.25 min	

Table 2.2: GC temperature program used for ground coffee samples.

	Temperature	Hold Time	Ramp Rate
Initial, T_1	50°C	1.00 min	10°C/min
T_2	235°C	5.50 min	

Table 2.3: Headspace and GC settings used for MeOH blanks and ground coffee samples.

Headspace Settings		MeOH Blanks	Ground Coffee
	Vial Equilibration Time	20.00 min	20.00 min
	Vial Fill Pressure	15 psi	15 psi
	Vial Size	20 mL	20 mL
	Sample Loop Injection Duration	0.50 min	0.50 min
	Loop Fill Rate	20 psi/min	20 psi/min
	Loop Final Pressure	10 psi	10 psi
	Loop Equilibration Time	0.05 min	0.05 min
	Loop Temperature	70°C	95°C
	Transfer Line Temperature	90°C	105°C
GC Settings			
	GC Cycle Time	37.00 min	40.50 min
	Split Ratio	1:1	1:1
	Split Flow	1 mL/min	1.1 mL/min
	Column Flow	1 mL/min	1.1 mL/min
	Column Pressure	7.7421 psi	8.8373 psi
	Average Flow Velocity	36.445 cm/s	38.223 cm/s

Discussion

3.1 Introduction

The analysis of volatile compounds in roasted coffee has been going on since the 1940s, when colorimetric tests were used in order to identify the compounds.[8] It wasn't until the 1950s that gas chromatography and mass spectrometry were implemented in the analysis.[9] Early on, gas chromatographs and mass spectrometers were developed with a fraction of the technology available today and it's amazing that the analytical methods involved in coffee flavour analysis have not changed much.

To date, there have been over 900 volatile compounds identified in roasted coffee. The complex mixture typically consists of, in order of most to least abundant: furans, pyrazines, ketones, pyrroles, phenols, hydrocarbons, acids and anhydrides, aldehydes, esters, alcohols, sulfur compounds and others.[10] Due to the complexity of the mixture and no specific analyte of interest, it is crucial to use GCMS, which is a suitable method that allows qualitative and quantitative analysis of as many compounds as possible.

3.2 The Maillard reaction

Flavours generated in food as a result of cooking are often products of the Maillard reaction.[11] When foods such as meat, bread, cookies, and onions are heated or

cooked, the naturally occurring amino acids and reducing sugars undergo nucleophilic substitution reactions, creating an array of caramelized and burnt flavours.[11] As the variety of amino acids and reducing sugars increases, so does the possible combination of Maillard reaction products. The combination of flavour compounds is also dependent on the time and the temperature at which the food is cooked, making the flavour profile of any cooked food unique.

3.3 Bridgehead collaboration

Bridgehead, an Ottawa-based coffee company, and known for their high quality coffee, noticed that their freshly roasted coffee would gradually lose its characteristic flavour over a period of months depending on the variety of coffee and the year it was cultivated. To illustrate the problem, one year, a particular batch of coffee may have lasted 8 months before turning, and in the following year, a new batch of that same variety of coffee may have lasted 10 months or 5 months. The shelf life of the green coffee beans could not be predicted, which often resulted in profit loss.

There are multiple factors that likely contribute to the chemical change in green coffee beans, including fermentation, moisture content, and oxidation.

After harvesting the coffee cherries, the depulped cherry pits remain coated with a thick gum-like residue called mucilage. Removing the mucilage is necessary to extract

the coffee beans and can be done by washing the pits with sodium hydroxide, mechanical scraping, or by fermentation, the latter being the most common removal method. Mucilage is naturally rich in polysaccharides and so it is broken down and consumed in the fermentation process. The fermentation commonly takes place in open vats of water that are exposed to the region's natural microorganisms, which then digest the mucilage.

Figure 3.1: Coffee cherries are fed into a series of rollers that compress the cherries, gently separating the cherry pits from the pulp.[12]

Figure 3.2: Beneath the pulp, the cherry pits are coated in mucilage. After removing the mucilage and milling away the parchment husk and the silver skin, the green coffee bean is shipped for roasting.[13]

Once the mucilage is removed, the pits or beans, still coated in their husk, are laid out to dry on a patio in the sun. The beans are moved around and turned repeatedly in order to dry them evenly. The drying step is complete when the beans have reached 10-12% moisture content, which is determined by feel and appearance. The beans are then packaged in moisture-controlled bags and shipped to a Bridgehead warehouse.

3.4 Data analysis

To begin developing methods, the experiments that could be considered involved either the green or roasted coffee beans. Though the change is taking place in the green beans, the impact of the change is more evident and more easily measured in the roasted coffee.

The three factors most likely to influence degradation of the green coffee beans are fermentation, moisture, and oxidation. After the beans are fermented to remove the mucilage, they are laid out in the sun to dry. Since the beans never undergo heat sterilization or irradiation, it may be possible that some microorganisms remain active. The beans are also dried to approximately 10-12% moisture content, which leaves water that may possibly sustain microorganisms. Finally, the beans are stored in moisture-controlled bags filled with air from the mill. This air may vary in humidity, carry airborne contaminants, and it certainly has oxygen. The oxygen in the air could oxidize and breakdown oils in the green beans, which would affect the flavours produced in the roasting process.

The roasted coffee contains many volatile compounds that give the brewed beverage its flavour. Since the taste and aroma of the coffee was gradually changing, monitoring the flavour profile over time seemed like the best thing to do. The initial hypothesis was that there would either be a trend of decreasing concentration of certain chemicals, or certain chemicals would increase in concentration, or both. The rough idea being that good flavours could be lost over time, while bad flavours could accumulate over time and this could be monitored with headspace GC-MS.

To begin the analysis, it was necessary to extract the volatile compounds from the coffee using various solvents in order to determine what was present and which solvents were effective. Ground coffee was extracted with cyclohexane, methanol, and

water. Each solvent extracted the same compounds and of the three, water was the most effective. In addition to extracting the ground coffee with solvents, the dry ground coffee beans were analyzed and the chromatographic peaks obtained were an order of magnitude higher in signal intensity.

From November 2016 to April 2017, five Guatemalan varieties of coffee were sample roasted and tested every couple of weeks. The coffees were brewed by following strict protocols made by Bridgehead. The coffee was coarsely ground consistently for brewing. During this period, the coffee was analyzed by sampling the ground beans and the brewed coffee. The headspace vials contained either 1.1 g of ground coffee or roughly 2 mL of brewed coffee. Because the relative percent abundance of each chemical was being measured, the exact sample quantities were not important to replicate. In analyzing both sampling methods, every possible peak that could be integrated was considered and only given a confirmed identity if the NIST database showed an 80% or higher match certainty with the mass spectrum. After collecting this data, it was found that both brewed and ground coffee showed no trends at all. Every single compound varied at random and did not show a gradual increase or decrease in abundance.

Table 3.1: Compounds identified in coffee via headspace GC-MS with a DB-WAX column.

Peak	Retention Time (min)	Chemical Name	Known Sensory Note	References
1	2.96	2-methylfuran	Spicy smoky	16
2	3.33	2-methylbutanal	Malty	14
3	3.72	2,5-dimethylfuran	Ethereal, Spicy smoky	14, 16
4	4.02	2-methyl-N-(2-methylpropyl)-1-propanamine		
5	5.00	2,3-pentanedione	Oily buttery, buttery	14, 15, 16
6	5.24	phenol	Smoky, sweet, tar	14, 16
7	5.95	2,3-hexanedione	Buttery, cheesy, sweet, creamy	14
8	6.08	3,4-hexanedione		
9	6.26	1-methyl-1H-pyrrole	Nutty, hay-like, herbaceous, smoky-tarry, diluted: sweet & woody	14, 16
10	6.32	4-methylphenol (p-cresol)		
11	6.86	pyridine	Bitter, astringent, roasted, burnt, penetrating odour, sharp taste	14, 16
12	7.31	pyrazine	Sweet, corn-like, nutty, spinach	16
13	7.34	1,3-diazine		
14	7.61	2-(methoxymethyl)-furan or furfuryl methyl ether	Nutty, coffee grounds-like, rich, phenolic, airy, roasted coffee	14, 16
15	7.71	3-methyl-3-buten-1-ol		
16	8.09	methylpyrazine	Nutty, roasted, chocolate, cocao, earthy	14, 16
17	8.32	4-methylthiazole	Nutty, green, roasted meat	16
18	8.65	N-nitrosodimethylamine		
19	8.88	2,5-dimethylpyrazine	Hazelnut, roasted, grassy, corn, nutty, cocao	14, 16
20	8.95	2,6-dimethylpyrazine	Nutty, sweet, fried, cocao, roasted nutty, roast beef	14, 16
21	9.07	ethylpyrazine	Nutty, roasted, musty, peanut butter	14, 16
22	9.23	2,3-dimethylpyrazine	Hazelnut, roasted, green, nutty, cocao-like	14, 15, 16
23	9.67	1-hydroxy-2-butanone		

Table 3.2: Continuation of compounds identified in coffee.

Peak	Retention Time (min)	Chemical Name	Known Sensory Note	References
24	9.74	2-ethyl-5-methylpyrazine	Nutty, roasted, grassy, roast	16
25	10.00	trimethylpyrazine	Nutty, roasted	14
26	10.53	3-ethyl-2,5-dimethylpyrazine	Potato, roasted, nutty	16
27	10.74	1-(acetyloxy)-2-propanone		
28	10.90	furfural	Bread, almond, sweet	14, 16
29	11.24	furfuryl formate		
30	11.39	2-(1-hydroxy-1-methyl-2-oxopropyl)-2,5-dimethyl-3(2H)-furanone		
31	11.46	2-Acetylfuran	Balsamic-sweet	14
32	11.72	2-furanmethanol acetate	Ethereal-floral fruity, fruity	16
33	12.35	5-methyl-2-furancarboxaldehyde	Almond, caramel, burnt sugar	16
34	13.02	1-methyl-1H-pyrrole-2-carboxaldehyde		
35	13.23	2-furanmethanol	Burnt	14
36	13.32	3-methylbutanoic acid		
37	14.09	N-acetyl-4(H)-pyridine		
38	15.34	1-(2-furanylmethyl)-1H-pyrrole	Hay-like, mushroom-like, green	14
39	15.69	2-methoxyphenol		
40	15.80	oxypurinol		
41	16.90	1-(1H-pyrrol-2-yl)ethanone (2-acetylpyrrole)	Nutty, musty	14
42	17.52	1H-pyrrole-2-carboxaldehyde		
43	17.64	2,4,7,9-tetramethyl-5-decyn-4,7-diol		
44	18.26	1-methyl-1H-pyrrole-2-carboxaldehyde		
45	18.59	nonanoic acid		
46	19.13	1-(2-hydroxy-5-methylphenyl)ethanone		

An attempt was made to extract some sort of trend from this data by matching the flavour compounds to their respective sensory notes, provided by literature. The compounds were then grouped and classified in terms of good and bad flavour

characteristics. It was hypothesized that the overall abundance of bad tasting flavours increased or the overall good tasting flavours decreased, but those claims would not have been well supported. Even though 31 flavour compounds could be identified and matched to a sensory note, many compounds varied a lot in relative percent standard deviation because they exist in such a minute quantity to begin with, making minor changes in percent abundance much more significant. As a result, the error bars were enormous and that analytical idea was set aside. In addition, judging whether the alleged sensory note was unpleasant or desirable would depend on potency and preference.

As time went on, the credibility of using a combination of individually matched sensory notes became questionable for describing or evaluating the coffee flavour. *d'Acampora Zellner et al.* used gas chromatography coupled with olfactometry to analyze flavour compounds in dairy products, coffee, and meat. As the chemicals were smelled using the olfactometer, sensory notes were assigned to describe the flavour aroma. Though some compounds were consistent in their description across different matrices, there were some compounds whose sensory notes differed substantially.

Table 3.3: Sensory note description of identical compounds in different food matrices.[17]

Compound	Sensory Note/Odour Description		
	In a meat sample	In a coffee sample	In a dairy sample
2,3-Pentanedione	Buttery, lemon, sweet, fruity	Buttery, oily	
2-Ethyl-3,5-dimethylpyrazine	Burnt, meaty, green	Nutty, roasted	
2-Methylbutanal	Pungent, green, sweet, roasty	Buttery, oily	
3-Methylbutanal	Pungent, green, sweet, roasty	Buttery, oily	Malt-like, green
Heptanal	Fatty, rancid, citric		Oily, fatty, sweet, nutty

It is apparent that not all chemical compounds possess a single set of characteristic sensory notes in varying food matrices. This could be due to the purity of the component being analyzed after leaving the GC. It's also likely that the concentration of certain flavour compounds vary between sample matrices, which could alter the way those chemicals are perceived. Nevertheless, the overall assessment of coffee quality by characterizing its flavour components has shown to be inconsistent and unreliable. It cannot be concluded that a single compound or a group of compounds are responsible for changing the quality of the coffee based on their individual sensory notes. To further complicate things, the flavour profile of the roasted coffee was always changing within the span of November 2016 to April 2017. There seemed to be no trend in anything that was being analyzed, and yet the coffee did not taste the same.

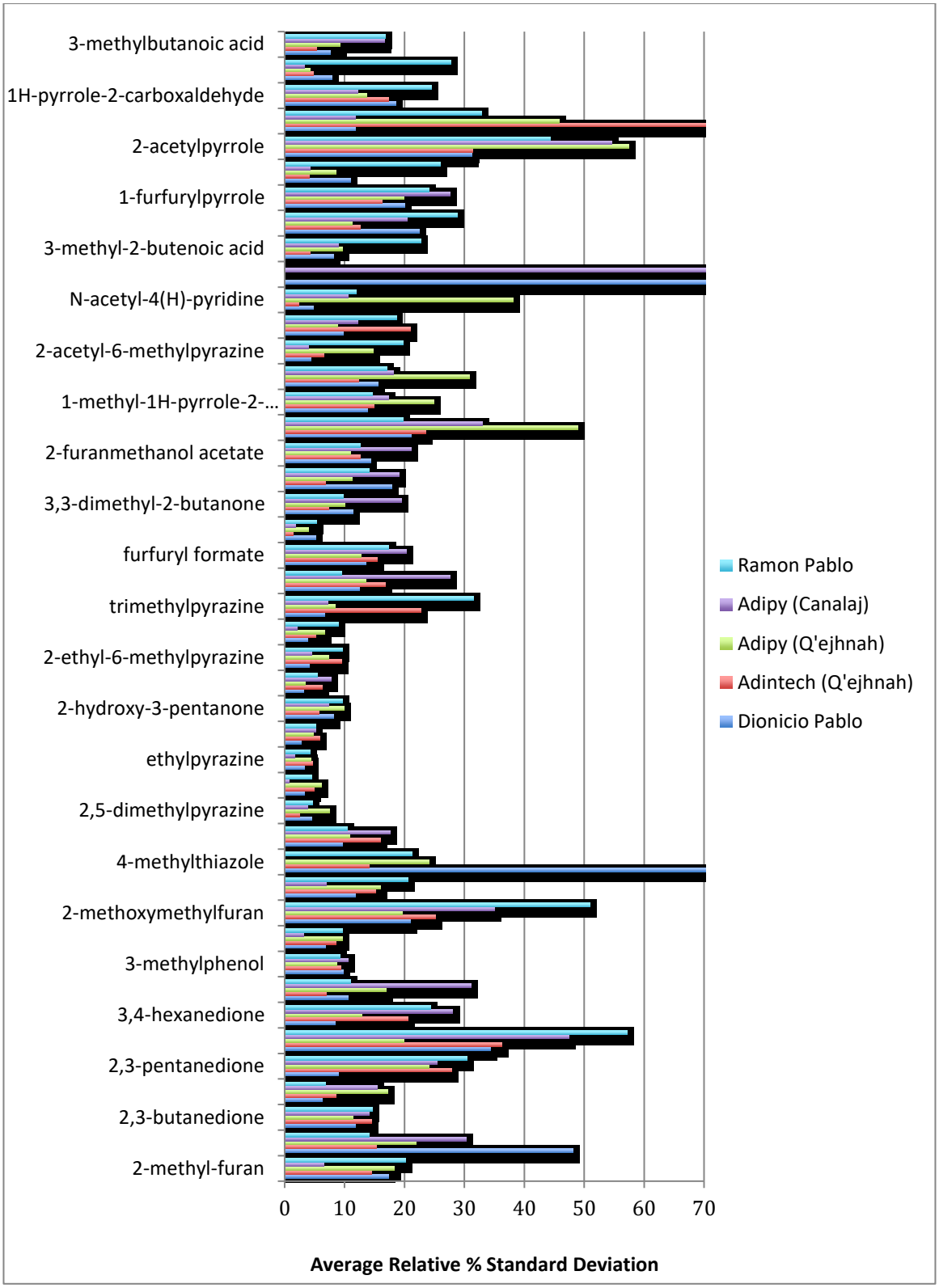

Figure 3.3: Average standard deviation with respect to the chemical's relative percent abundance in the five coffee varieties analyzed from November 2016 to April 2017.

Running with the idea that the flavour profile of the roasted coffee is always changing, a new hypothesis was pursued regarding the non-uniform aging of the green beans. The idea being that each individual coffee bean varies slightly in shape and size. This would affect the water content, since the differently sized beans would not have been dried to an identical percent humidity. During storage, the beans with higher humidity content could support fermenting species or simply depreciate at different rates than a smaller, dryer bean. The way each bean roasts individually would also differ slightly. Higher moisture content would slow down the initial roasting because the heat would be transferred to the water before roasting the bean. This would mean that each batch of ground coffee is an average of coffee beans that varied in depreciation and then were roasted to various degrees.

To test this hypothesis, each coffee being analyzed was roasted three times and then each of the three roasts were analyzed in triplicates. The variation in the triplicates would suggest error in the analysis technique, whereas the variation in the three roasts would suggest error in the roasting. The prediction was that over time, the green coffee beans would depreciate at different rates while in storage. As the green beans depreciate non-uniformly, the diversity or deviation within the green bean sample would increase, which would be reflected in the roasted coffee. With time, more and more green beans would depreciate and their roasted product would contain less of the unique flavours that initially made the coffee so desirable. If all this were true, then the variation in the roasts should increase over time. This was not the case.

Table 3.4: Average percent standard deviation of the relative chemical abundances from September 2017 to June 2018.

Coffee Variety	Sept 2017	Jan 2018	Apr 2018	Jun 2018
Cielito Lindo	5.41%	3.14%	3.52%	2.79%
Ramon Pablo	3.58%	3.89%	N/A	5.25%
Adipy Lot 5	3.02%	4.50%	6.05%	4.21%
Adintech Lot 16	5.15%	4.63%	6.56%	10.77%

After sampling the same four coffees in September 2017, January 2018, April 2018, and June 2018, the average percent standard deviations of the relative chemical abundances were inconsistent. By June 2018, the sensitivity of many compounds became too low and those compounds were no longer being detected. All the data from this set was normalized over the period from September 2017 to June 2018, considering only species that were identified in all samples within the coffee variety being analyzed. The relative percent abundance of a compound was determined from summing the peak areas of all compounds within the normalized data set.

The hypothesis was that over time, roasting the green beans would generate less consistent flavour profiles, resulting in higher deviations in chemical abundance between roasting batches. This hypothesis was made with emphasis on the possibility of microorganism activity on or within the green beans. It is possible that the humidity of the beans all gradually reached equilibrium with the humidity level inside the moisture-

controlled bag and may have not supported microbial activity as easily as originally thought.

Noticing that more and more chemicals were dropping below detectable limits over time, the peak intensities from September 2017 to June 2018 were compared.

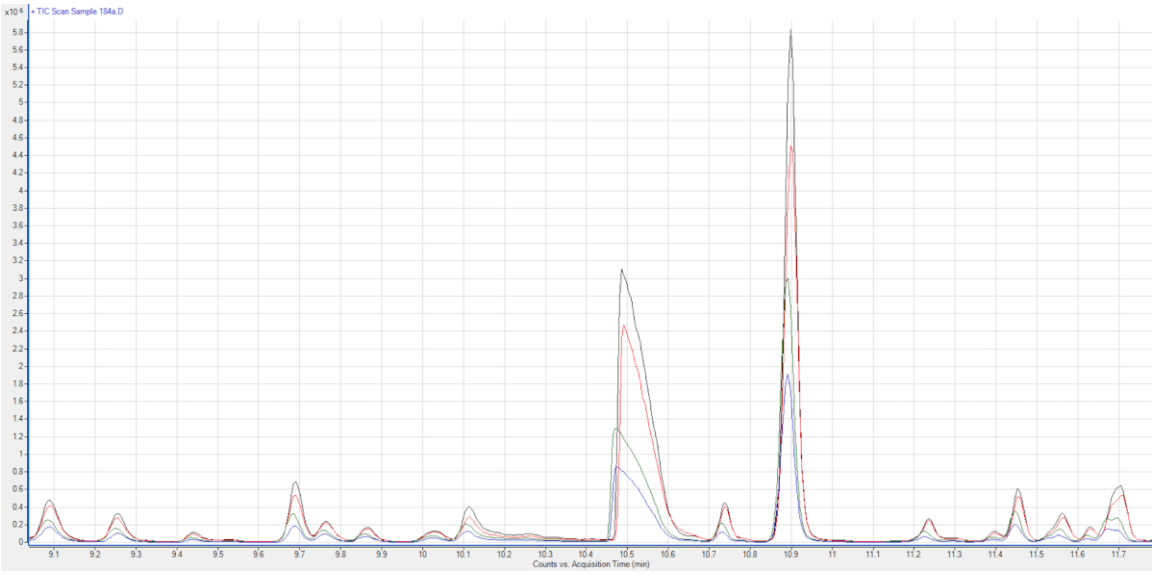

Figure 3.4: A snap shot of overlaid chromatograms of the same coffee type showing a gradual decrease in signal intensity in order of highest to lowest from September 2017 to June 2018. This data was collected from the Adintech Lot 16 roasted coffee samples.

It appeared as though the data in this figure showed levels of volatile species decreasing over time by a factor of about 150. Unfortunately, this compelling result was quickly halted after finding data for standards that had been run on the same instrument within the same time period. The cyclohexanol and cyclohexanone impurities in a cyclohexane solvent showed the same 150-fold decrease in sensitivity. Since the solvent

was taken from the same cyclohexane bottle, the concentrations of the impurities should have remained constant, which suggests a loss of sensitivity for the instrument.

Though it was disappointing that this data could not be used to draw conclusions, it supports exactly what is being investigated: a loss of volatile components attributing to unique flavours. The aroma that each roasted coffee sample gave off changed significantly over the course of the four time points. In September 2017, the buttery and fruity, sometimes chocolate flavours could be sensed in the freshly ground coffee. By June 2018, all four coffees smelled the same and no longer had those aromas that originally made them unique.

3.5 Conclusion

It was found that the flavour components within roasted coffee varied randomly from November 2016 to April 2017. Between September 2017 and June 2018, the flavour components still varied randomly and the rate at which they varied was neither consistent nor change progressively within all coffee types. The most promising result suggested that the volatile components of the roasted coffee had decreased from September 2017 to June 2018 by a factor of 150, but then it could not be proved that this result was not attributed to the instrument's loss in sensitivity.

After smelling the freshly ground roasted coffee of the four different varieties from September 2017 to June 2018, it is very obvious that the aroma and flavour profile changes significantly. The final method of comparing peak intensity over time may still be an optimistic approach, however the sensitivity of the instrument should not be in question.

3.6 Future works

Degradation of green coffee beans after prolonged storage is likely a major factor influencing the quality of the roasted product. It was found that the concentration of volatile species in the roasted coffee declined significantly over a period of several months. In future work, this trend would prevail, but may not be easily exploited for the company's financial gain.

Should this research be continued, monitoring the peak intensity of volatile compounds would be a great place to start. Incorporate an internal and external standard consistently in order to accurately measure loss of sensitivity by the instrument.

The benefit of measuring the concentration of volatile species is that the change over time can be recorded as a numerical value as opposed to a human memory. The recorded values can be monitored and evaluated as the concentration decreases. Once the roasted coffee reaches a point where its unique flavours are no longer perceived, the concentrations at that moment could be set as a threshold. Future coffee sample measurements could then be compared to the threshold values when evaluating their quality status at any point in time. Though this method could work for a coffee batch in stock, it can only help with monitoring the status of the coffee over time.

In terms of predicting the rate at which coffee will degrade before purchasing it, this method cannot help predict anything. The rate at which coffee degrades varies with coffee type, seasons, and many more complex factors. Also, the rate of degradation is often non linear, which means there is currently no easy way of predicting coffee quality in the future months to come.

It may be of interest to study biological activity of the green beans prior to purchasing. If there is an unusual amount of microbial growth, it could possibly validate the instability of the green beans.

3.7 References

1. Tswett, M. S. *Proceedings of the Warsaw Society of Naturalists in Biology*, **1905**, vol. 14, no. 6, 20-39.

2. Archer John Porter Martin. Encyclopedia of Life Sciences [Online]; Wiley & Sons, Posted 2001. http://onlinelibrary.wiley.com/store/10.1038/npg.els.0002871/asset/a0002871.pdf?v=1&t=jbzc9fqy&s=f700ad730375957d456f30387d5297e8c2ccc760 [accessed Jan 3, 2018]

3. Evolution of Gas Chromatography. http://www.labmanager.com/lab-product/2010/02/evolution-of-gas-chromatography (accessed Jan 3, 2018).

4. Tipler, A. *An Introduction To Headspace Sampling In Gas Chromatography*; PerkinElmer, Inc.: Massachusetts, 2013; pp 15.

5. Agilent Technologies. https://www.chem.agilent.com/cag/cabu/gccolchoose.htm#Material (accessed December 20, 2017)

6. Shrader, S. *Introductory Mass Spectrometry*, 2nd ed.; CRC Press: Florida, 2014; pp 8-11.

7. Shimoda, M.; Shibamoto, T. *J. Agric. Food Chem.* **1990**, *38*, 802-804.

8. Hughes, E. B.; Smith, R. F. *J. Soc. Chem. Ind*., **1949**, *68*, 322-327.

9. Zlatkis, A.; Sivetz, M. *J. Food Sci.*, **1960**, *25*, 395-398.

10. Toledo, P. R. A. B.; Pezza, L.; Pezza, H. R.; Toci, A. T. *Comprehensive Reviews in Food Science and Food Safety*. **2016**, *15*, 705-719.

11. Capuano, E.; Ferrigno, A.; Acampa, I.; Ait-Ameur, L.; Fogliano, V. *Eur Food Res Technol*. **2008**, *228*, pp 228.

12. rijo42, a coffee supplier in the UK. https://www.rijo42.co.uk/blog/rijo42-coffee-beans-journey-commercial-coffee-machines

13. National Coffee Association of U.S.A., Inc. http://www.ncausa.org/About-Coffee/10-Steps-from-Seed-to-Cup

14. Yang, N.; Liu, C.; Degn, T. K.; Munchow, M.; Fisk, I. *Food Chemistry*. **2016**, *211*, 206-214.

15. Toledo, P. R. A. B.; Pezza, L.; Pezza, H. R.; Toci, A. T. *Comprehensive Reviews in Food Science and Food Safety*. **2016**, *15*, 705-719.

16. Steen, I.; Waehrens, S. S.; Petersen, M. A.; Münchow, M.; Bredie, W. L. P. *Food Chemistry*. **2017**, *219*, 61-68.

17. d'Acampora Zellner, B.; Dugo, P.; Dugo, G.; Mondello, L. *J. Chromatogr. A*. **2008**, *1186*, pp 123-143.

Part II – Mechanistic exploration into methylation enhancement of phospholipids using diazomethane

Introduction

4.1 Mass spectrometry

4.1.1 History and development of mass spectrometry

Amongst his many scientific discoveries, Sir J. J. Thomson investigated the positively charged rays (anode rays) that were first discovered by Eugen Goldstein in 1886. Thomson shined a narrow beam of the positively charged rays onto a photographic plate. Prior to hitting the plate, he subjected the beam to an electrical force and a magnetic force, acting perpendicularly to one another. Thomson figured out that the particles of the same mass in the beam struck the photographic plate at some point, depending on their velocity, on a parabolic curve. This was the birth of the first mass spectrometer. After overcoming many challenges with his initial design, Thomson acquired the first mass spectra of gaseous mixtures inside his discharge tube. [18, 19]

As well as proving the existence of hydroxide radicals, using his mass spectrometer, Thomson analyzed neon gas, known for its red glow in advertising signs. He was able to separate ^{20}Ne and ^{22}Ne based on their mass to charge ratio. Thomson had successfully performed the first isotopic separation.[18]

4.1.2 How it works

4.1.2.1 Ionization source

4.1.2.1.1 Electron ionization

Electron ionization sources are used in the analysis of small molecules that have boiling points below 300°C. This source is enclosed and typically coupled with the gas chromatograph, since it is only effective under high vacuum and with very low solvent concentrations, if any.

In GCMS, the analyte molecules exit the column and pass through an ionizing electron beam prior to entering the single quadrupole mass analyzer. The electron beam is generated by a heated tungsten filament. When passing a current through the heated filament, electrons are emitted as they are drawn towards a positive potential, set on an electron trap plate. As the analyte molecules pass through the beam of electrons, the molecules are ionized, fragmented, and then separated in the quadrupole. The energy of the electron beam is set universally at 70 eV, which is considerably higher than typical bond energies. As a result, the electron beam generally forms more fragment ions than intact molecular ions, and so the ionization technique is referred to as hard. The electron impact source also generates positively charged ions almost exclusively, since electrons are ejected from the analyte molecules. Because protonation does not occur in electron ionization, the ions have the same mass as the molecular fragment, as oppose to the M+H peaks in ESI spectra.

4.1.2.1.2 Electrospray ionization

Electrospray ionization was first published in 1988 by John B. Fenn. He later won half the 2002 Nobel Prize in Chemistry for his discovery. Electrospray operates by forcing an analyte solution through an open-ended capillary to form an aerosol spray. The spray consists of charged analyte within solvent clusters. The solvent clusters are broken up by inert desolvation gas, typically nitrogen. A relatively small fraction of ions get past the opposing curtain gas, which is nitrogen, and make it to the orifice.

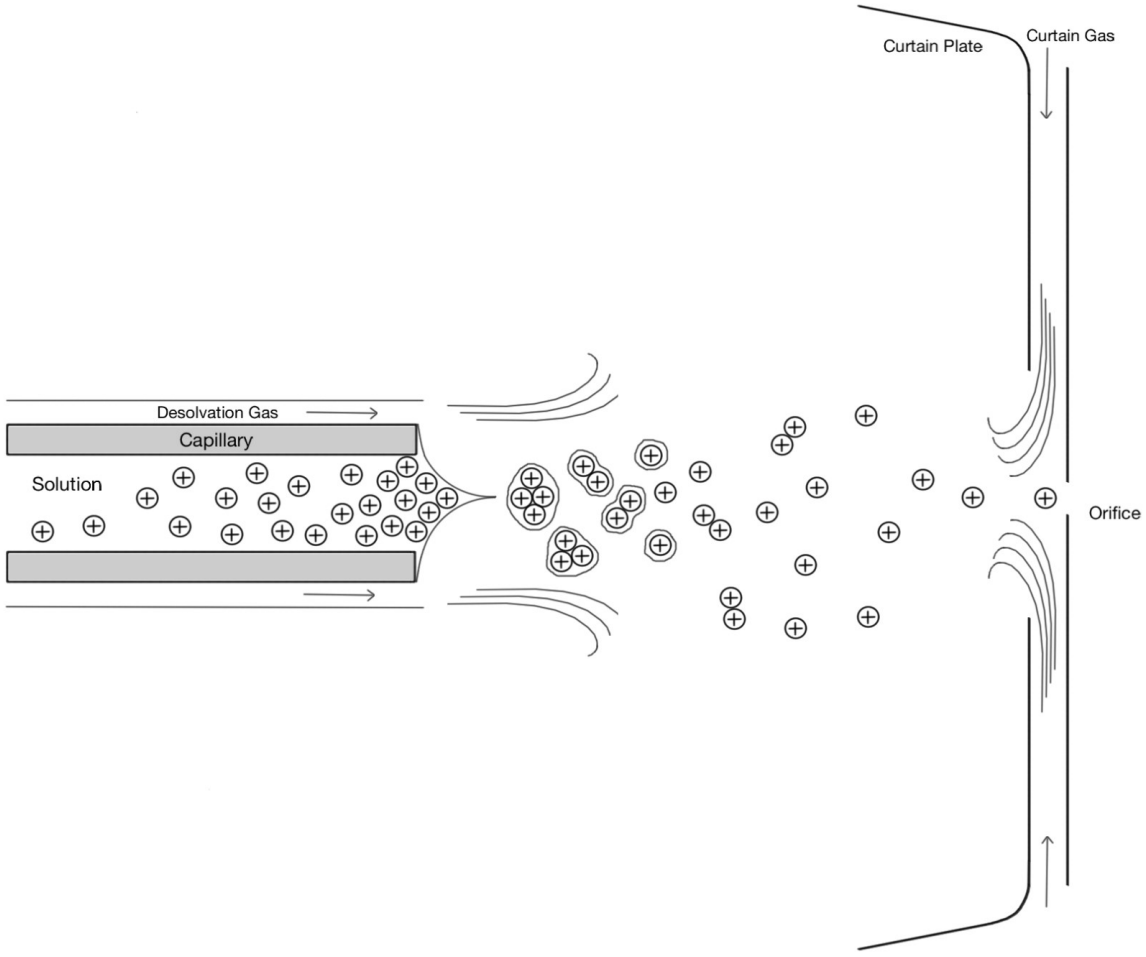

Figure 4.1: Electrospray ionization source.

Nanospray incorporates the same theory of electrospray on a nano scale. Disposable nanospray tips are small glass capillaries that are closed to a very fine, and pointed tip. The fine tip must be gently flexed and broken to create a very small opening for the analyte solution to spray. In order to withstand an applied voltage of +1000 V, the nanospray tips are coated with gold and palladium. The metal coating acts as a conductive surface and has a very high oxidation potential.

4.1.2.2 Quadrupole mass analyzer

The ions are accelerated through an increasing potential difference towards the quadrupole for separation and detection. The quadrupole is comprised of four gold plated stainless steel rods, precisely aligned in a square configuration. The four rods manipulate the electromagnetic field in order to separate the incoming ions based on their mass to charge ratio, which is denoted as m/z in units of Thompsons.

The quadrupole focuses the ions by applying both positive and negative DC voltages to the rods. The positive rods are opposite each other and the negative rods are opposite each other. The rod pairs switch polarity at MHz frequencies, which causes the ions to focus in a tight corkscrew-like path. To separate the ions within the beam, a resonating frequency is applied to offset all mass to charge ratios except those within a small range. The ions that differ by more than 0.05 Th from the selected ion oscillate

with amplitude that destabilizes their trajectory such that only the selected ion flies toward the detector. When the resonating frequency is changed, so does the "selected ion", and so ions of varying mass to charge ratios can be detected sequentially in a single scan by varying resonating frequencies.

4.1.2.3 Time of flight detector

The ions enter the ToF in packets via a valve connecting the mass analyzer portion of the instrument. The packet of ions fly temporarily next to a repeller plate, which pulses the ions in a drift-free path, perpendicular to the path of entry. The ions separate in the flight tube based on the kinetic energy imparted to them, which is related to their mass to charge ratio. As the ions reach the opposite end of the drift tube, they enter an ion mirror or reflectron. The reflectron is typically made up of around 50 metal plates set to progressively increase in voltage to create a potential gradient. The plates surround the flight path of the ions and reflect the ions by decelerating, then accelerating them towards the detector. The time required for each ion to hit the detector is measured at GHz frequencies, which results in a very accurate and precise measurement.[20]

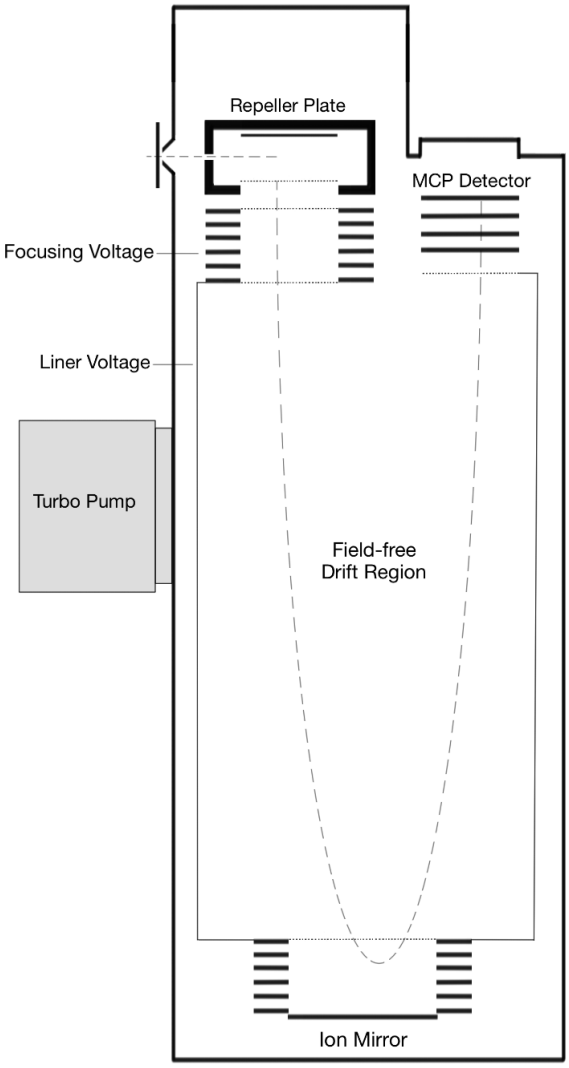

Figure 4.2: Time of Flight Detector

4.1.3 Why mass spectrometry is the best

Mass spectrometry is an ideal method of analysis for all experiments. It can confirm the analyte structure by showing a fragmentation pattern that is unique to that particular analyte. The fragments can be modeled and grouped together to suggest

molecular structures, which can help identify byproducts and show insight to reaction pathways. High-Resolution mass spectrometers are capable of detecting the exact mass of an ion to 0.0001 Da, which enables structural confirmation with a high level of certainty.

Using the nanospray tips to directly spray a reaction mixture into the mass spectrometer is very convenient. These tips are advantageous for samples that can offer kinetic related data immediately following the reaction or for samples that degrade over time. The direct spray method can also show an undisturbed reaction mixture, which can provide insight regarding the reaction dynamics. The nanospray tips are also disposable, which means that no cleaning is required and the risk of contamination is minimized.

Quadrupole mass analyzers offer a robust and reliable separation of ions. However, they lack the sensitivity of an ion trap because ions are separated based on only allowing a specific m/z ratio to pass through. As a result, most of the ions are ejected from the rods and a small percentage of ions actually move towards the detector.

The Time of Flight is a detector with high-resolution capabilities and greater sensitivity than the quadrupole mass analyzer. When the ion packets enter the ToF, the ions are accelerated simultaneously and then separated based on their kinetic energy

before hitting the detector. Detecting all the ions that leave the quadrupole is how the ToF prevents further loss of sensitivity.

4.2 Analysis of biometabolites

4.2.1 Classes of phospholipids

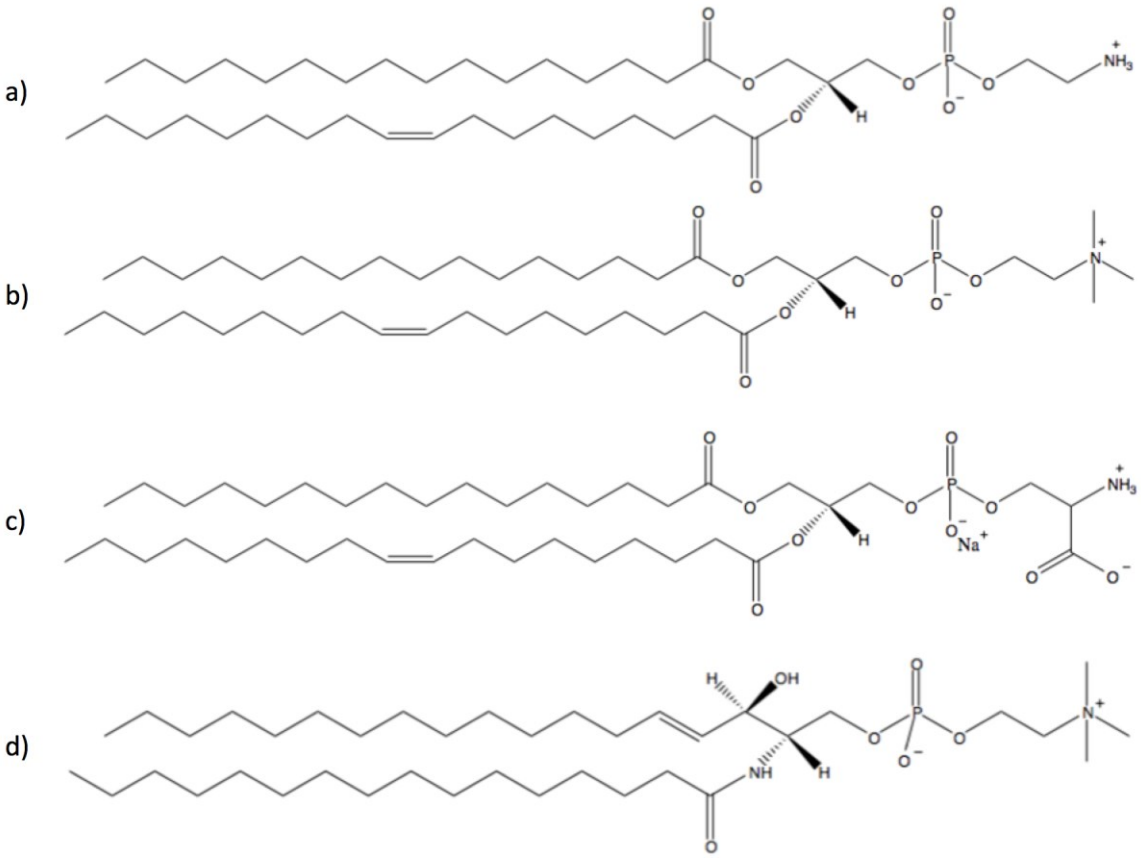

Figure 4.3: The four most abundant classes of phospholipids in mammalian cell membranes: a) Phosphatidylethanolamine (PE), b) Phosphatidylcholine (PC), c) Phosphatidylserine (PS), d) Sphingomyelin (SM).

Phospholipids are a class of lipids with prominent roles in mammalian cell membranes. Types of phospholipids vary in the polar head group and the backbone moiety connecting the head group to the fatty acids.

4.2.2 Importance of phospholipid analysis

Phospholipids are believed to play a prominent role in mammalian cell function. They are present in the cell membrane and the organelles within cells. Since their abundance varies depending on the function of the tissue, of the organelle, and of the organ, it is clear that phospholipids serve a greater purpose than just a structural membrane component.[21] PC is the most abundant phospholipid in mammalian cell membranes and accounts for 40-50% of total phospholipids.[21] It acts as a second messenger in signal transduction and is also the most prevalent phospholipid in bile, lung surfactant, and plasma lipoproteins.[22] PE is the second most abundant phospholipid in mammalian cells, accounting for 20-50% of total phospholipids.[21] PE is found in brain tissues and its content in mitochondria is much higher compared to other organelles. PS is found in brain tissues and in retina[21] and SM plays a particularly important role in the health of placental tissues.[23] Though PS and SM are relatively less abundant phospholipids in membranes, they are concentrated within regions of specific cellular function. For this reason, it is important to investigate the functionality of phospholipids within cell tissues in order to elucidate potential causes and treatments of diseases.

4.2.3 Application of lipidomics to overcome analytical difficulties

Phospholipids are prone to coordinating with salt or potentially existing as neutral species in solution. In addition to the immense variety of lipids in a cell membrane, this makes phospholipid quantitation for tissue samples very difficult using mass spectrometry. The discrepancy from neutral phospholipids in solution as well as signal splitting caused by protonated and sodiated phospholipid species results in lower signal intensity.

Using diazomethane to methylate phospholipids in solution protects acidic sites and prevents the exchange of protons with sodium. This modification also fixes a positive charge to thrice-methylated amine moieties; thereby assuring that the lipid species remains charged in solution. This better assures that when the solution is sprayed, the analyte will fly more easily and reliably in the gas phase towards the mass spectrometer. As a result, methylation of phospholipids, using diazomethane, improves signal intensity by increasing the ionizability of the analyte and by unifying split signals to form one peak.[24, 25]

Materials and methods

5.1 Materials

Solvents:

Ethanol (100%) was purchased from Commercial Alcohols. Methanol and diethyl ether were purchased from Fisher Scientific.

Reagents:

Potassium hydroxide was purchased from Fisher Scientific. Boron trifluoride diethyl etherate was purchased from Sigma Aldrich.

Lipid Standards:

Sphingomyelin (16:0), Phosphatidylethanolamine (16:0, 18:1), and Phosphatidylcholine (16:0, 18:1) were purchased from Avanti Polar Lipids, Inc. individually as pure standards in chloroform.

Equipment:

Disposable 9" Pasteur pipettes were purchased from Fisher Scientific. NanoES spray capillaries were purchased from Thermo-Fisher Scientific. Fused silica tubing (200μm ID, 354μm OD) was purchased from Polymicro Technologies. PEEK tubing (1/16"

OD, 0.010” ID) was purchased from Supelco. The PEEK fittings used to assemble the base and the diazomethane gas lines were purchased from SciPro.

5.2 Methods

Methylation reaction general method:

In a glass pipette vial, 50 μL of 100 μM lipid in MeOH or EtOH was methylated in roughly 300 μL solvent and 0-10 μL of 100 μM HBF_4 in MeOH or EtOH. The diazomethane vial consisted of 216 mg *N*-Nitroso-*N*-methylurea, 3 mL 8.9M KOH(aq), and 2 mL water. The base was injected quickly through a 20G needle into the diazomethane vial. The diazomethane was fed into the lipid solution at room temperature through a 0.010” ID PEEK line connected by a 20G needle in the diazomethane vial and an 18G needle in the lipid solution.

Mass spectrometry sample preparation:

An 8 μL aliquot of sample containing 15 μM lipid in MeOH or EtOH was injected into a NanoES spray capillary and spun in a centrifuge. The capillary was then scored with a ceramic cutter and snapped above the solvent meniscus. The capillary was then inserted into the conductive ferrule at the ESI source and gently tightened. The capillary tip was then flexed against the curtain plate to fracture and ideally, break it off to facilitate spraying the sample.

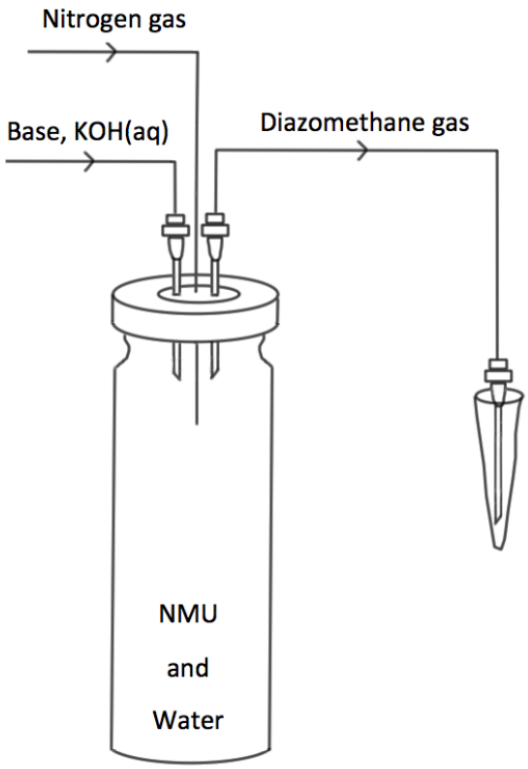

Figure 5.1: Schematic of the diazomethane bubbler apparatus

Instrument settings:

Table 5.1: AB Sciex QSTAR QToF nanospray instrument settings.

Source/Gas		
	Ion Source Gas 1	3
	Curtain Gas	20
	IonSpray Voltage	1000-1100 V
Compound		
	Declustering Potential	65 V
	Focusing Potential	265 V
	Declustering Potential 2	15 V
	Collision Gas	2
Detector		
	Channel Electron Multiplier	2200.0 V

Discussion

6.1 Diazomethane

Diazomethane is used as an effective methylating agent. The main advantages of diazomethane are that it can be produced as a gas in situ from stable starting materials and the only byproduct formed in the methylation reaction is nitrogen gas, making it a very clean reaction.

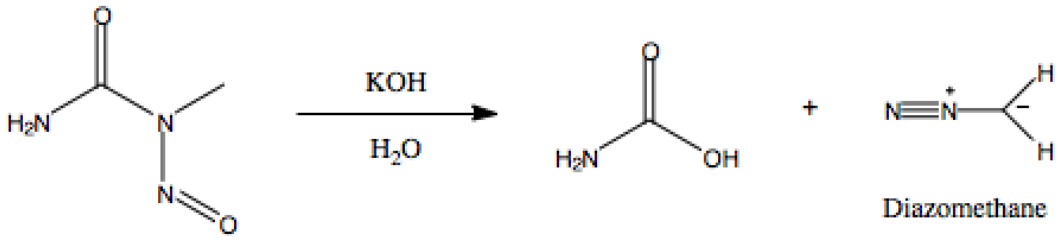

Figure 6.1: Production of diazomethane from N-Nitroso-N-methylurea.[26, 27]

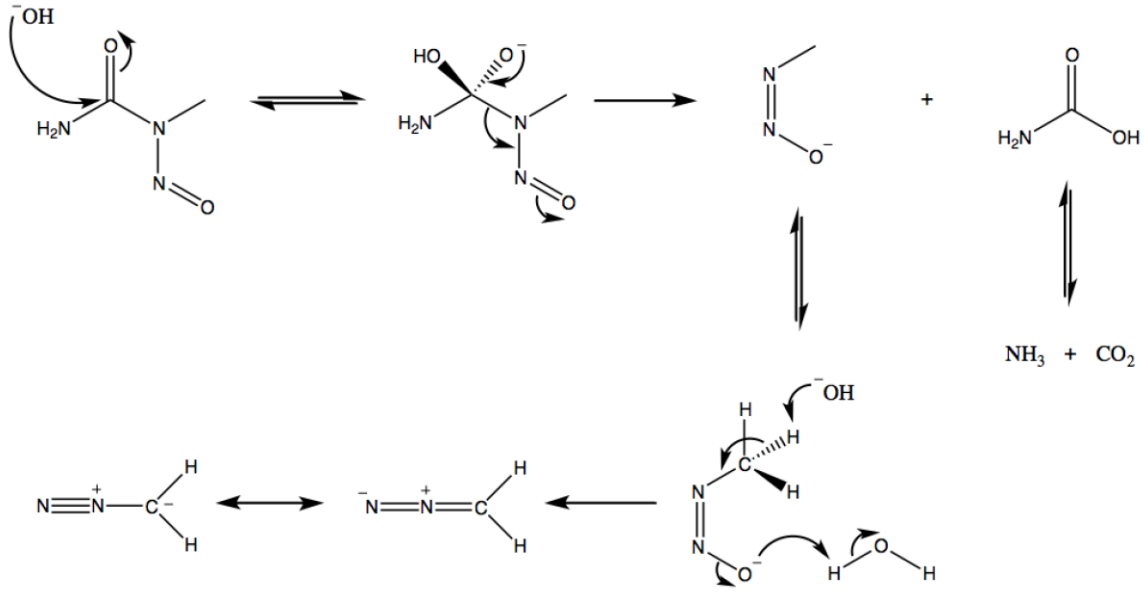

Figure 6.2: Base-catalyzed formation of diazomethane mechanism.[28]

N-Nitroso-*N*-methylurea undergoes base hydrolysis when mixed with 8.9 M KOH(aq) and water. The reaction produces carbamic acid and diazomethane gas.

As a methylating agent, diazomethane acts in a two-step process. The nucleophilic carbanion first deprotonates an acidic moiety, then following the deprotonation, the conjugate base acts as a nucleophile and attacks the electrophilic methyl group.

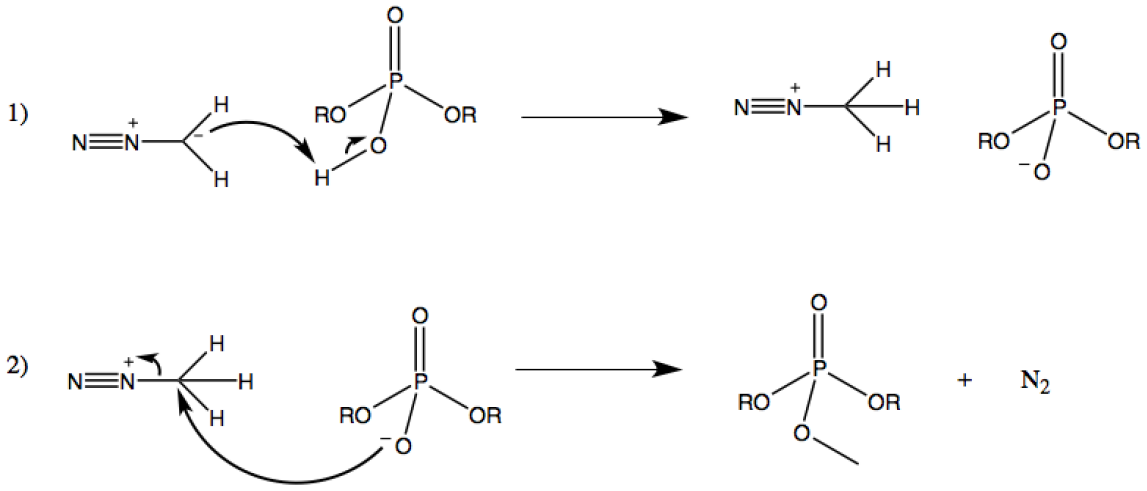

Figure 6.3: Diazomethane as a methylating agent.

6.2 Results

6.2.1 Ethanol complex formation causes peak splitting

A fresh 100μM PE standard was prepared in EtOH. The mass spectrum of this standard is shown in figure 6.4.

In a glass pipette vial, 50 μL of 100μM PE standard was methylated in 300 μL EtOH without HBF_4. The diazomethane vial consisted of 207 mg *N*-Nitroso-*N*-methylurea, 1 mL ether, and 3 mL 8.9M KOH(aq). This reaction produced mostly thrice methylated PE with m/z 760 (protonated) and 782.5 (sodiated) and a very small amount of four times methylated PE with m/z 774.5 (protonated). The reaction also produced other unknown species in a considerable amount with m/z 811.5 and 825.5. This mass spectrum is shown in figure 6.5.

In an attempt to convert the previously reacted PE to four times methylated (fully modified), the lipid reaction solution was diluted with 100 μL EtOH and a second round of diazomethane was bubbled through the PE solution at room temperature. The diazomethane vial consisted of 3 mL water, 215 mg *N*-Nitroso-*N*-methylurea, 1 mL ether, and 3 mL 8.9M KOH(aq). As shown in figure 6.6, this reaction produced more of the unknown species with m/z 811.5 and 825.5 instead of fully modified PE.

The same apparatus was set up, but using fused silica lines instead of the PEEK lines in an attempt to not produce the unknown species with m/z 811.5 and 825.5. In a glass pipette vial, 50 μL of 100μM PE standard was methylated in 200 μL EtOH without HBF_4. The diazomethane vial consisted of 3 mL water, 205 mg *N*-Nitroso-*N*-methylurea, 1 mL ether, and 3 mL 8.9M KOH(aq). The diazomethane was fed into the lipid solution at room temperature through a fused silica line. Figure 6.7 shows that this reaction produced a mixture of once methylated PE with m/z 732.5 (protonated) and 754.5

(sodiated), thrice methylated PE with m/z 782.5 (sodiated), and four times methylated PE with m/z 774.5 (protonated). The reaction also produced the unknown peaks with m/z 811.5 and 825.5. This result demonstrates that the PEEK lines are not the cause of the unknown species. It also shows that the PEEK lines are more effective and efficient than the fused silica at methylating PE under these conditions.

Because the reaction occurs at room temperature, the ether evaporates and passes from the diazomethane vial and into the lipid solution. Ether is very good at solvating diazomethane in solution and it is also miscible with EtOH, so it was originally believed that ether would improve the efficiency of the methylation reaction. However, to assure the ether was not contaminating the reaction, the reaction was attempted without ether.

In a glass pipette vial, 50 μL of 100μM PE standard was methylated in 300 μL EtOH without HBF_4. The diazomethane vial consisted of 3 mL water, 207 mg *N*-Nitroso-*N*-methylurea, no ether, and 3 mL 8.9M KOH(aq). As shown in figure 6.8, this reaction produced mostly thrice methylated PE with m/z 760 (protonated) and 782.5 (sodiated) and a very small amount of four times methylated PE with m/z 774.5 (protonated). The reaction also produced the unknown species with m/z 811.5 and 825.5.

At this point, the only components of the entire apparatus are KOH, water, diazomethane, PE, and EtOH. Water vapour does condense on the inner wall of the

diazomethane vial, but not enough to suggest a substantial amount is being carried over through the PEEK line. Diazomethane is too unstable to form any species other than its decomposition products: carbamic acid, a methyl group and nitrogen gas. This means the 811.5 and 825.5 adducts must involve some type of EtOH species. To test this hypothesis, the PE standard was dried down to evaporate the EtOH and then resuspended in MeOH.

A 50 μL aliquot of 100μM PE standard in EtOH was dried down and resuspended in 300 μL MeOH and transferred to a glass pipette vial to be methylated. The diazomethane vial consisted of 3 mL water, 221 mg *N*-Nitroso-*N*-methylurea, no ether, and 3 mL 8.9M KOH(aq). As shown in figure 6.9, this reaction produced mostly four times methylated PE with m/z 774.5 (65.7%), some thrice methylated PE with m/z 760.5 and 782.5 (combined 28.9%), and a small amount of the enolate adduct species with m/z 811.5 (5.4%) from residual EtOH that didn't evaporate.

The enolate complex supposedly being formed may be controversial, considering that diazomethane is commonly shown in literature to be a weak base. The formation of the complex suggests that diazomethane is removing a hydride from EtOH, a hydride having a pKa around 48. The formation of this complex is heavily supported by mass spectrometry data, contradicting current theory. The proposed mechanism, depicted in figure 6.10, shows the EtOH being attacked twice by two separate diazomethane molecules. Figure 6.11 shows the rearrangement of the m/z 577.5 fragment and figure

6.12 shows the proposed rearrangement of the m/z 135 enolate fragment, both of which are found in the msms of the m/z 811.5 and m/z 825.5 fragments. Finally, figures 6.13 and 6.14 depict the product ion scans for the m/z 811.5 and m/z 825.5 fragments, respectively, and figures 6.15 and 6.16 depict their fragmentation patterns, respectively. After considering the puzzle explained by these mass spectra, it appears as though diazomethane behaved unconventionally under methylation conditions that were not acid catalyzed.

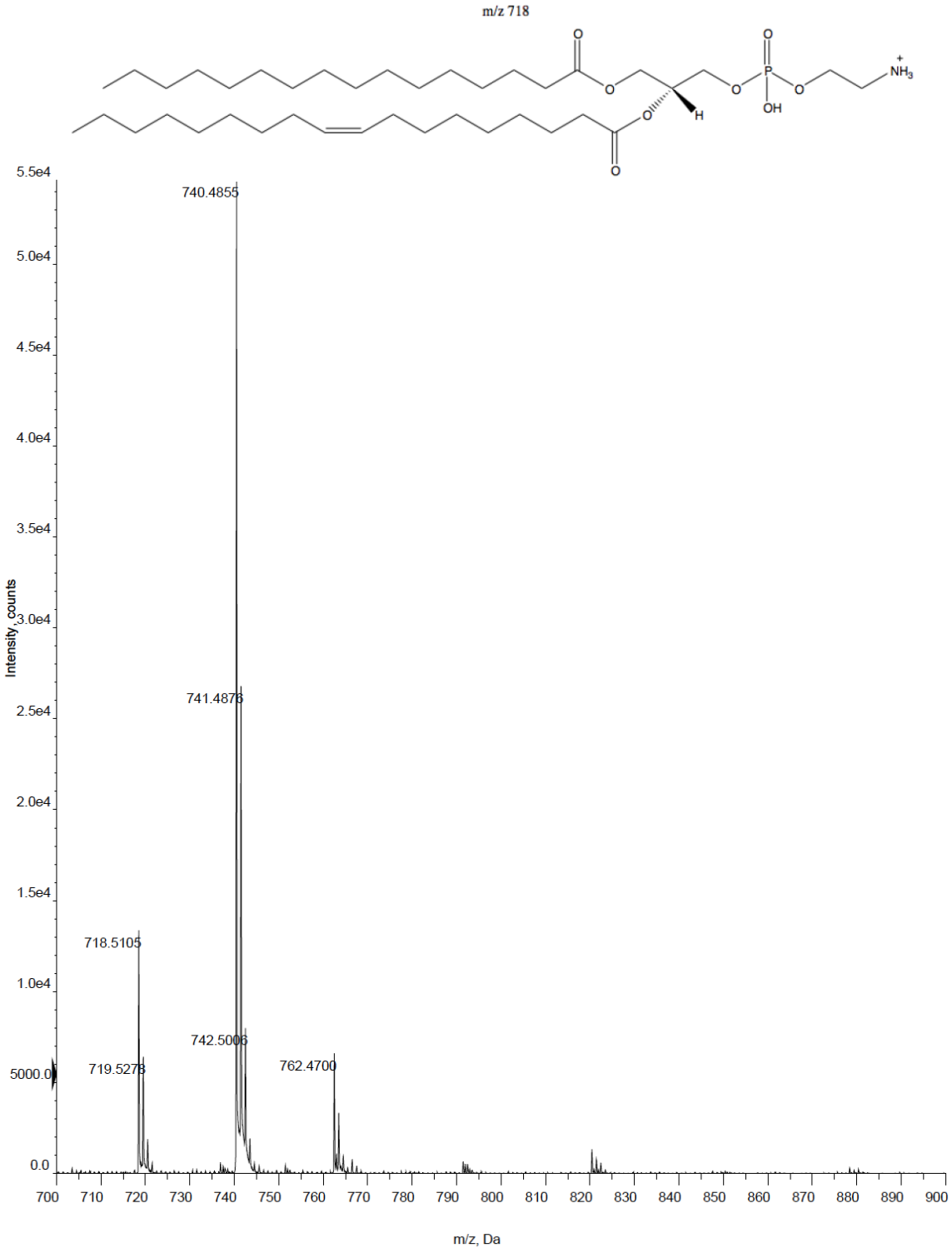

Figure 6.4: Unmodified 100µM PE standard in EtOH.

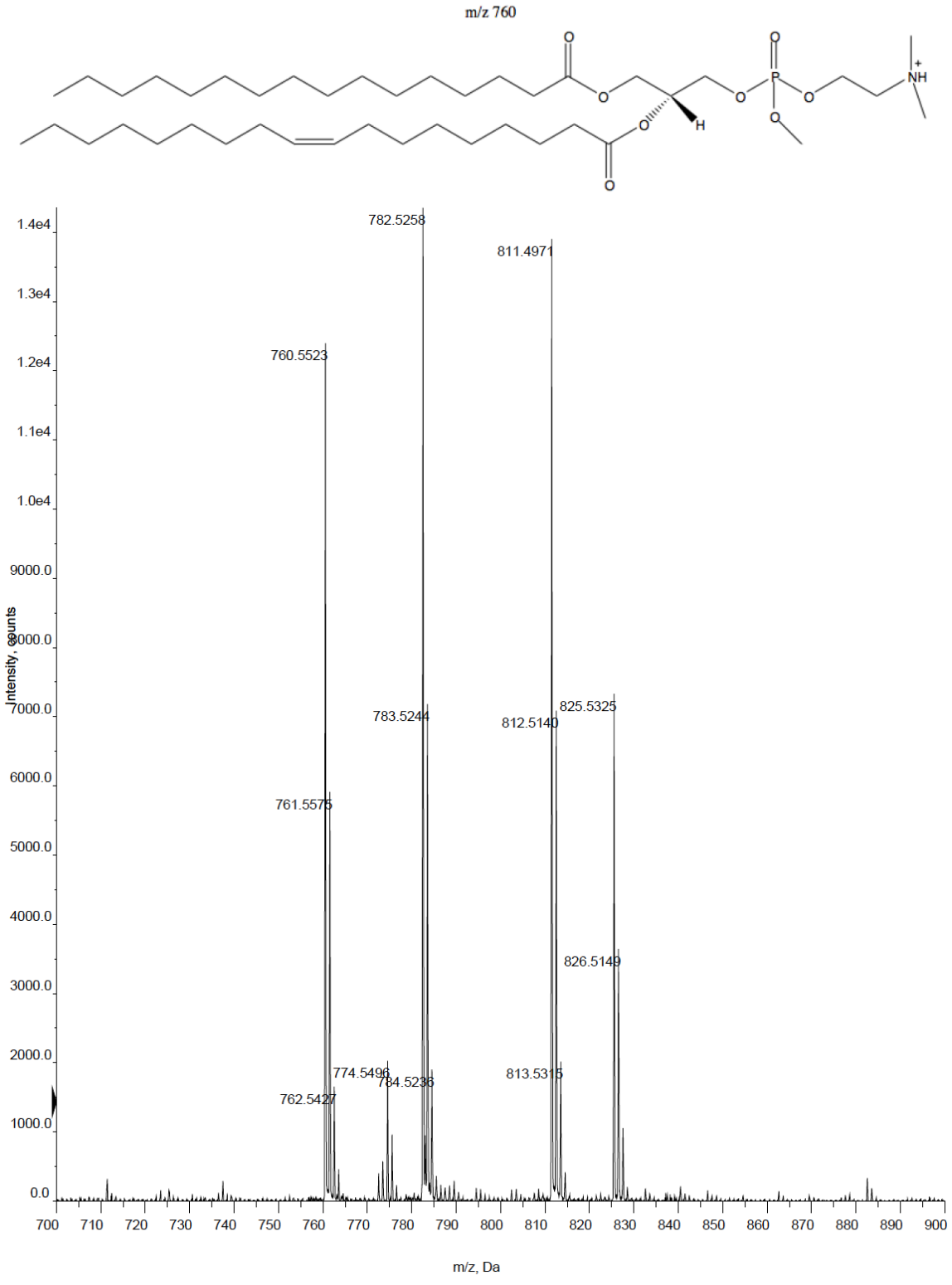

Figure 6.5: PE methylation after one round of diazomethane with ether and no HBF_4.

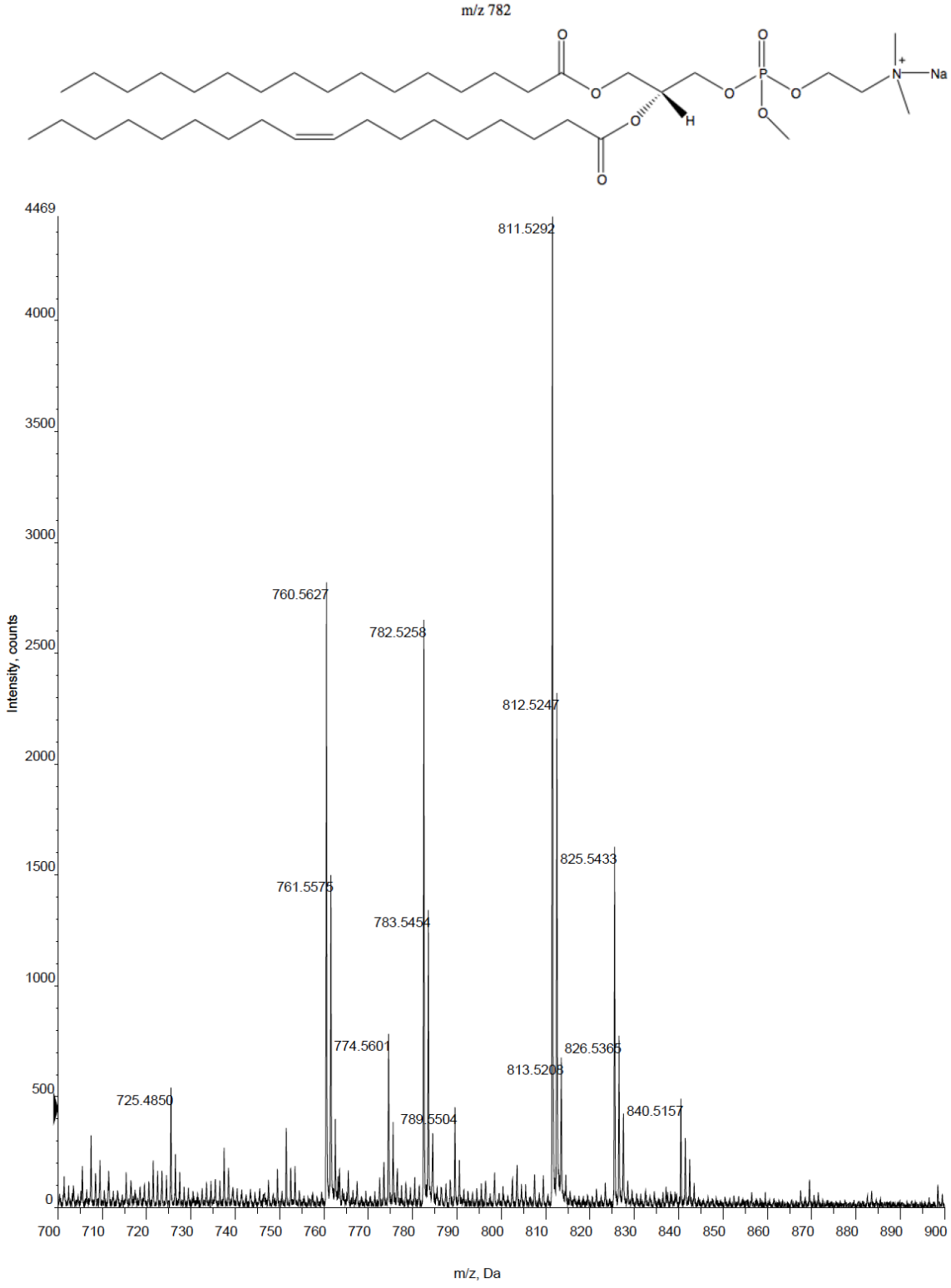

Figure 6.6: PE methylation after two rounds of diazomethane with ether and no HBF_4.

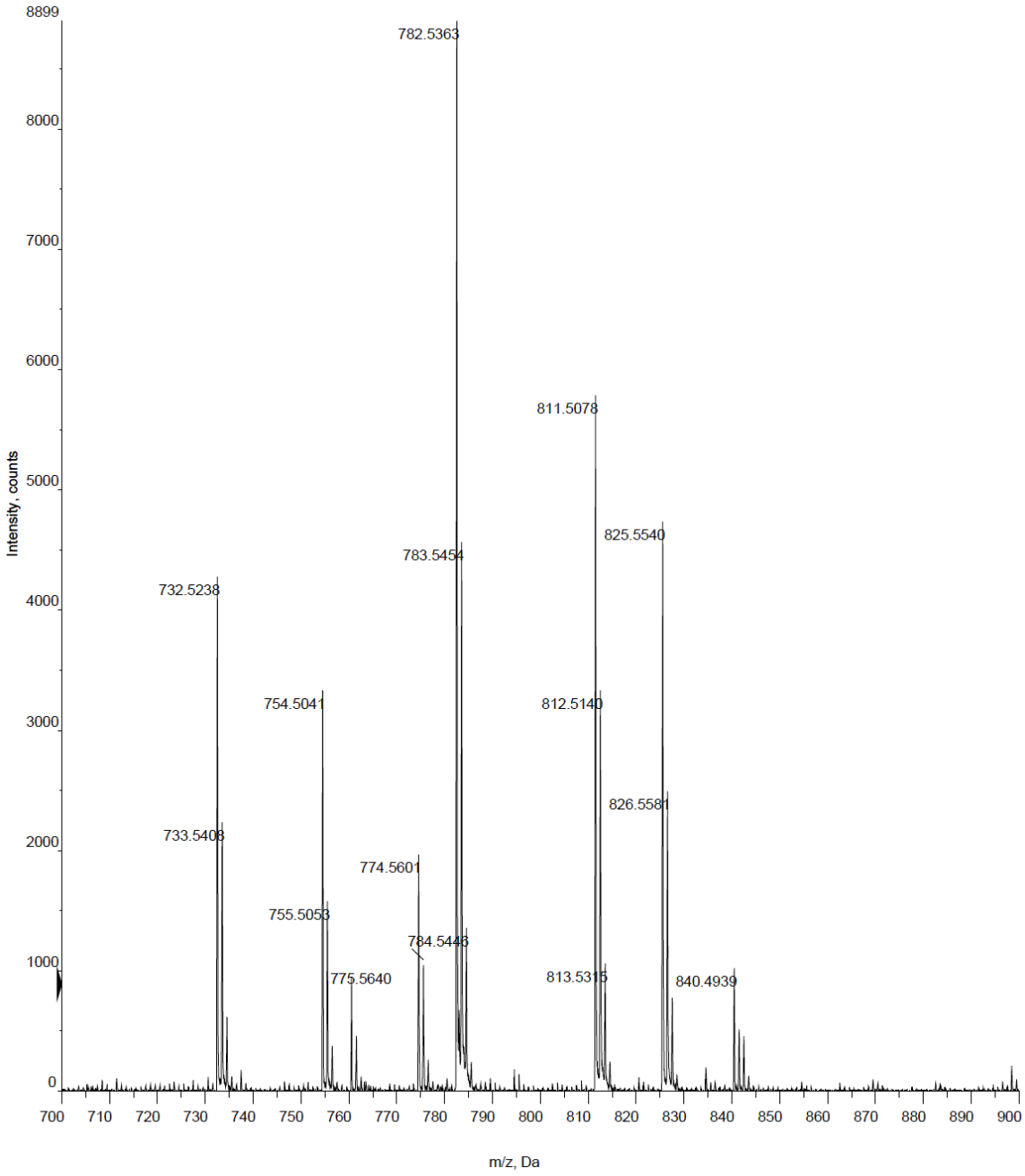

Figure 6.7: PE methylation with ether and no HBF_4, using fused silica lines.

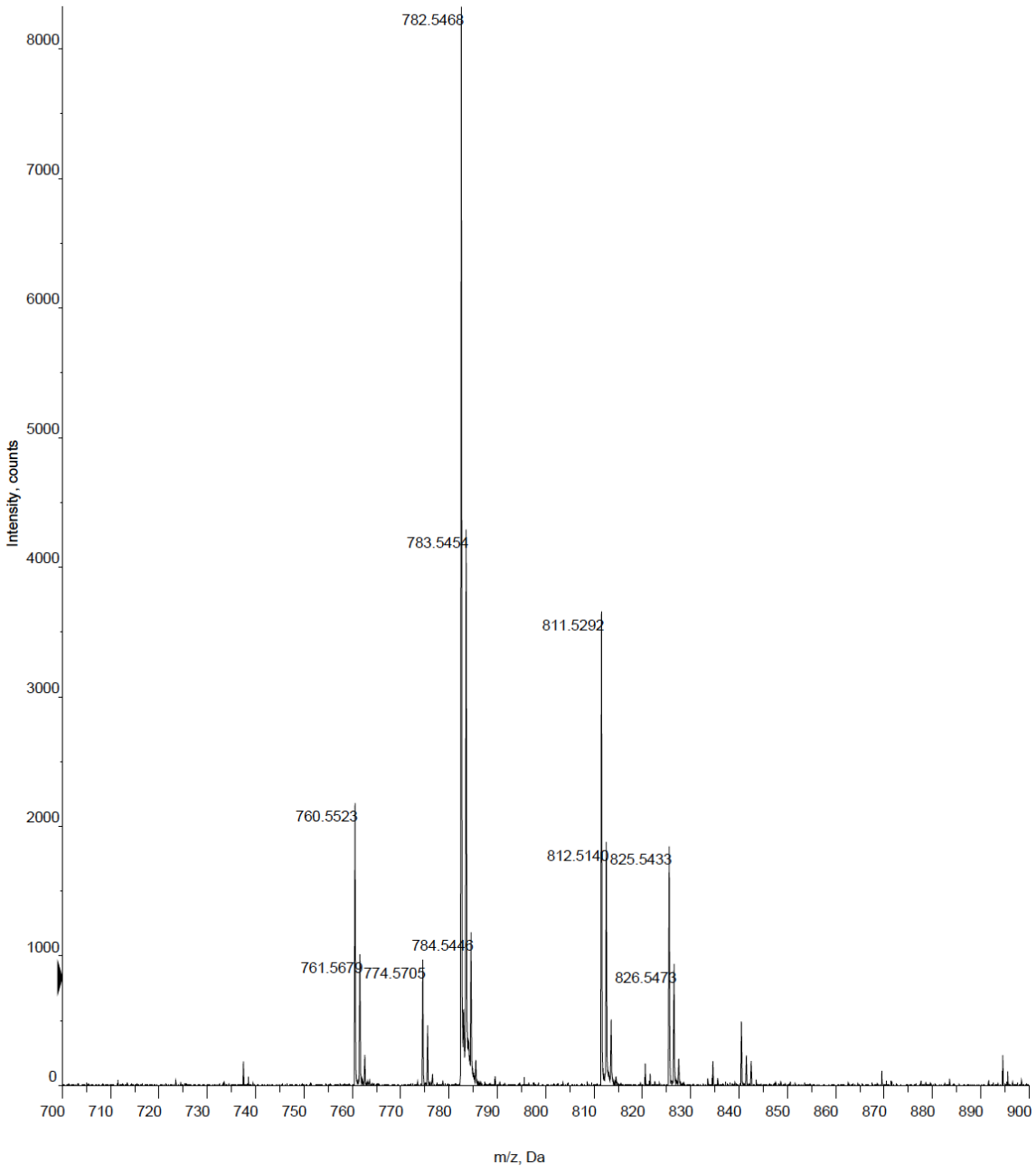

Figure 6.8: PE methylation with no ether and no HBF_4.

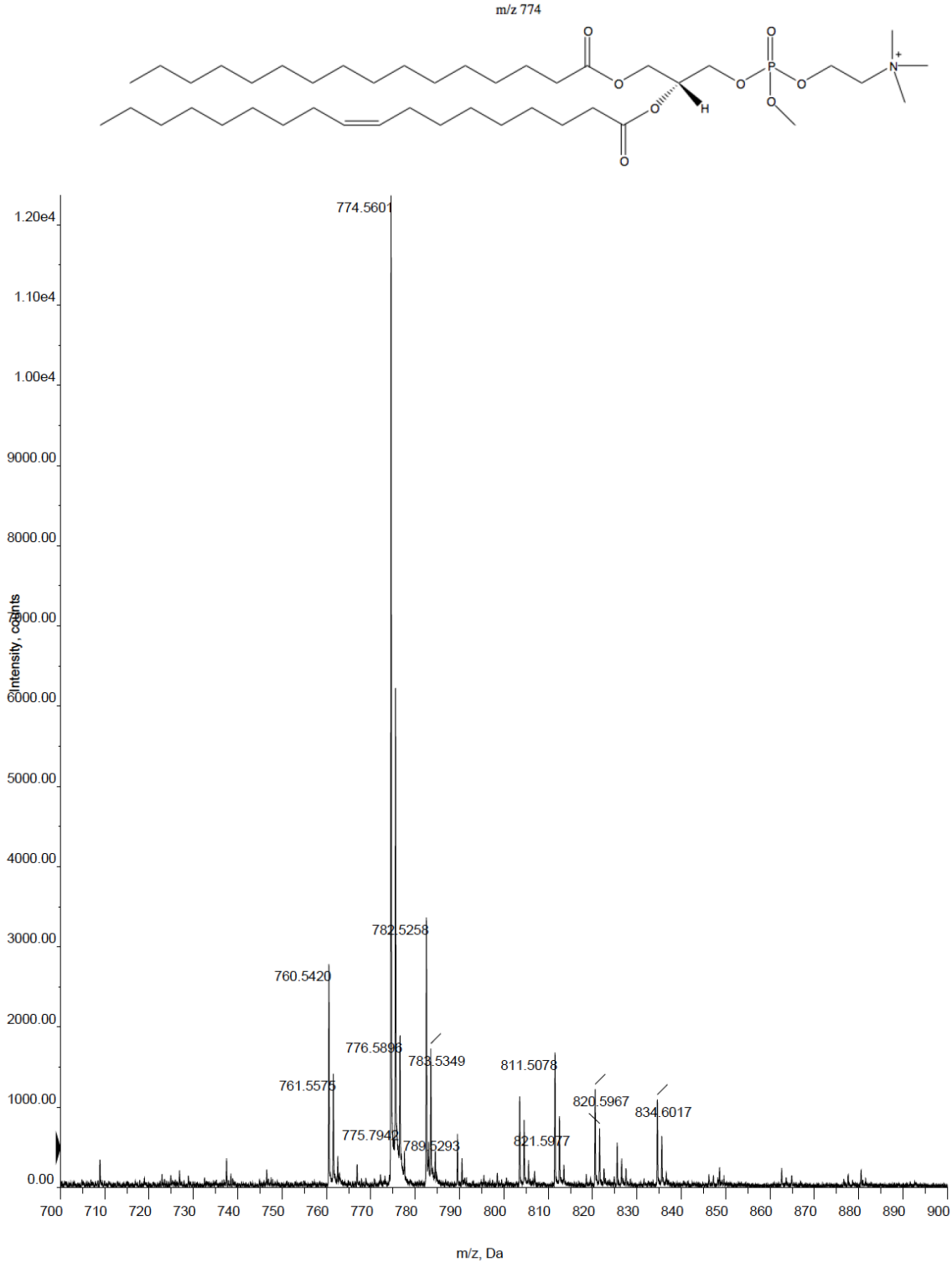

Figure 6.9: PE methylation in MeOH with no ether and no HBF_4.

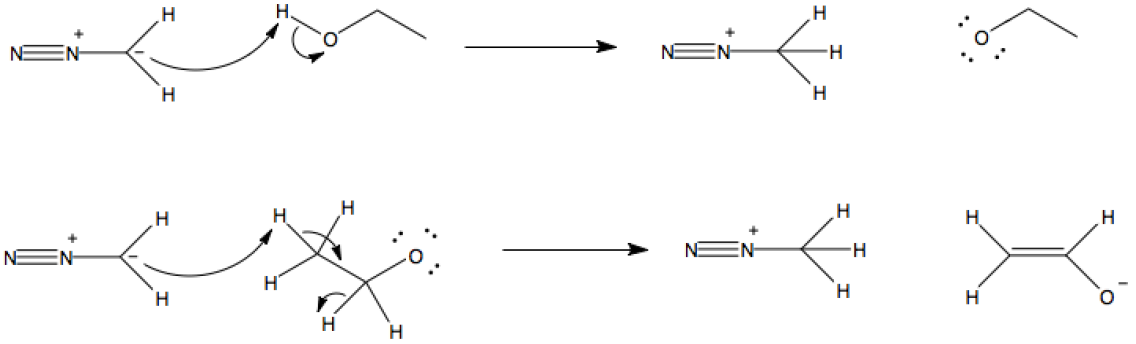

Figure 6.10: Suggested mechanism for the formation of enolate via diazomethane.

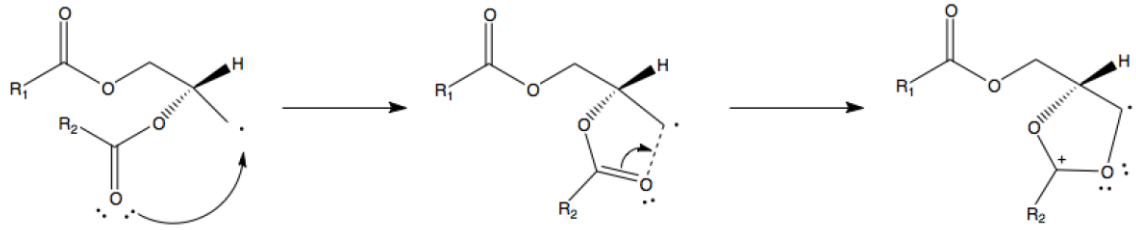

Figure 6.11: Rearrangement mechanism for the m/z 577.5 fragment ion formation.

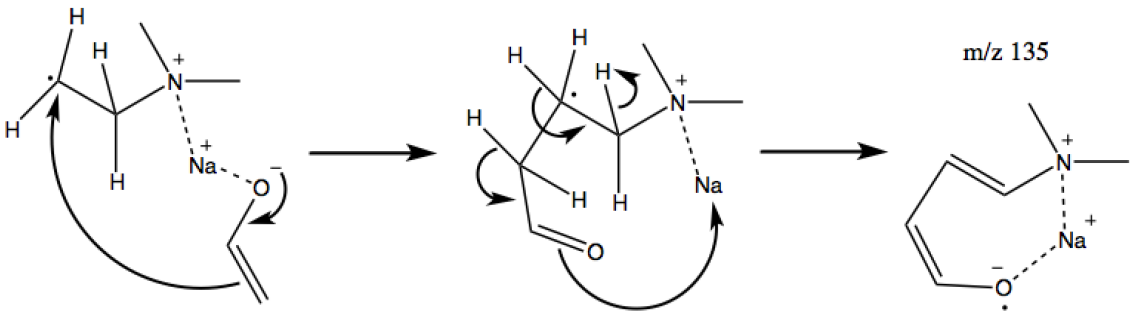

Figure 6.12: Suggested rearrangement mechanism for the m/z 135 enolate fragment ion formation.

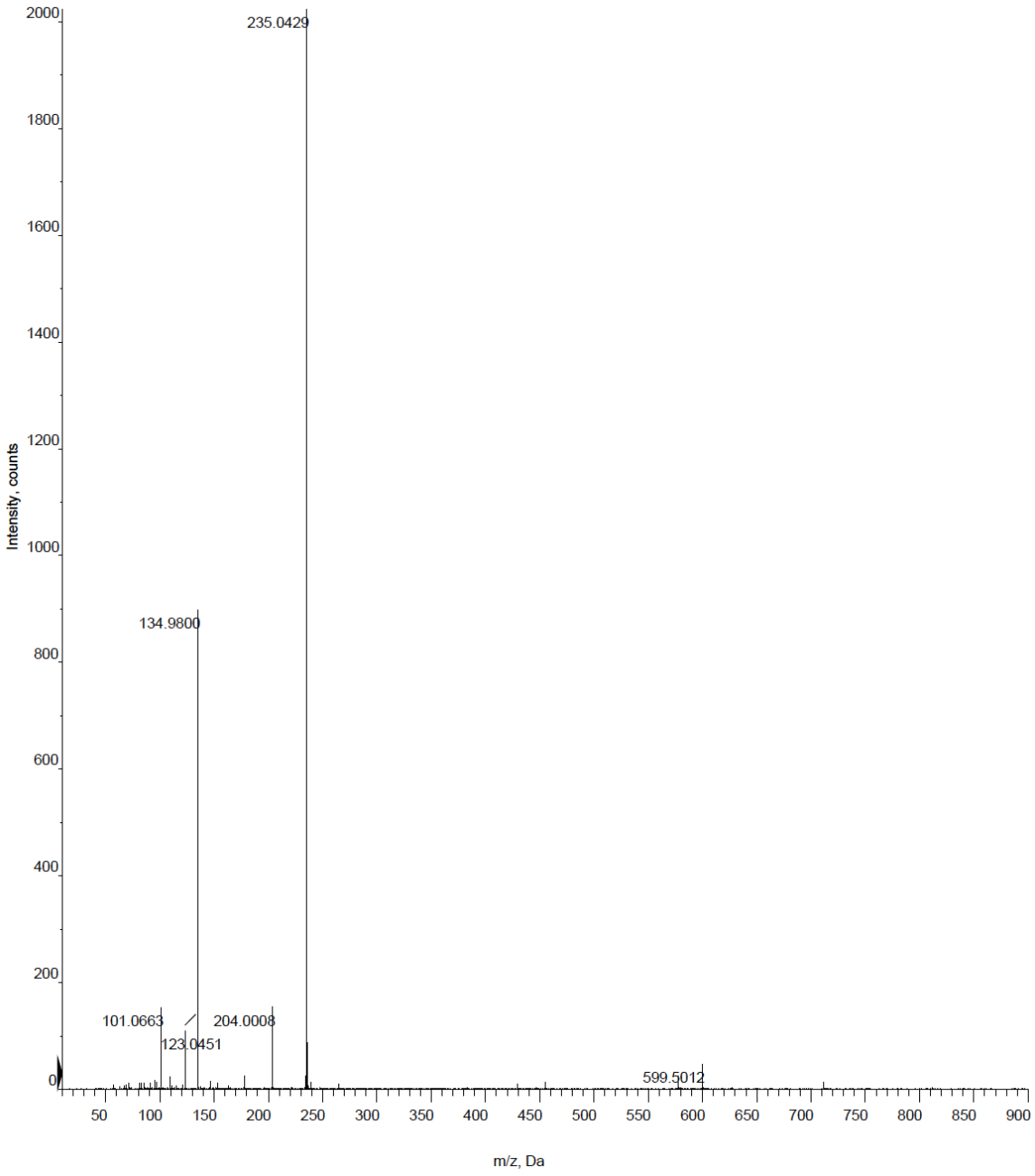

Figure 6.13: The product ion scan of the m/z 811.5 fragment ion.

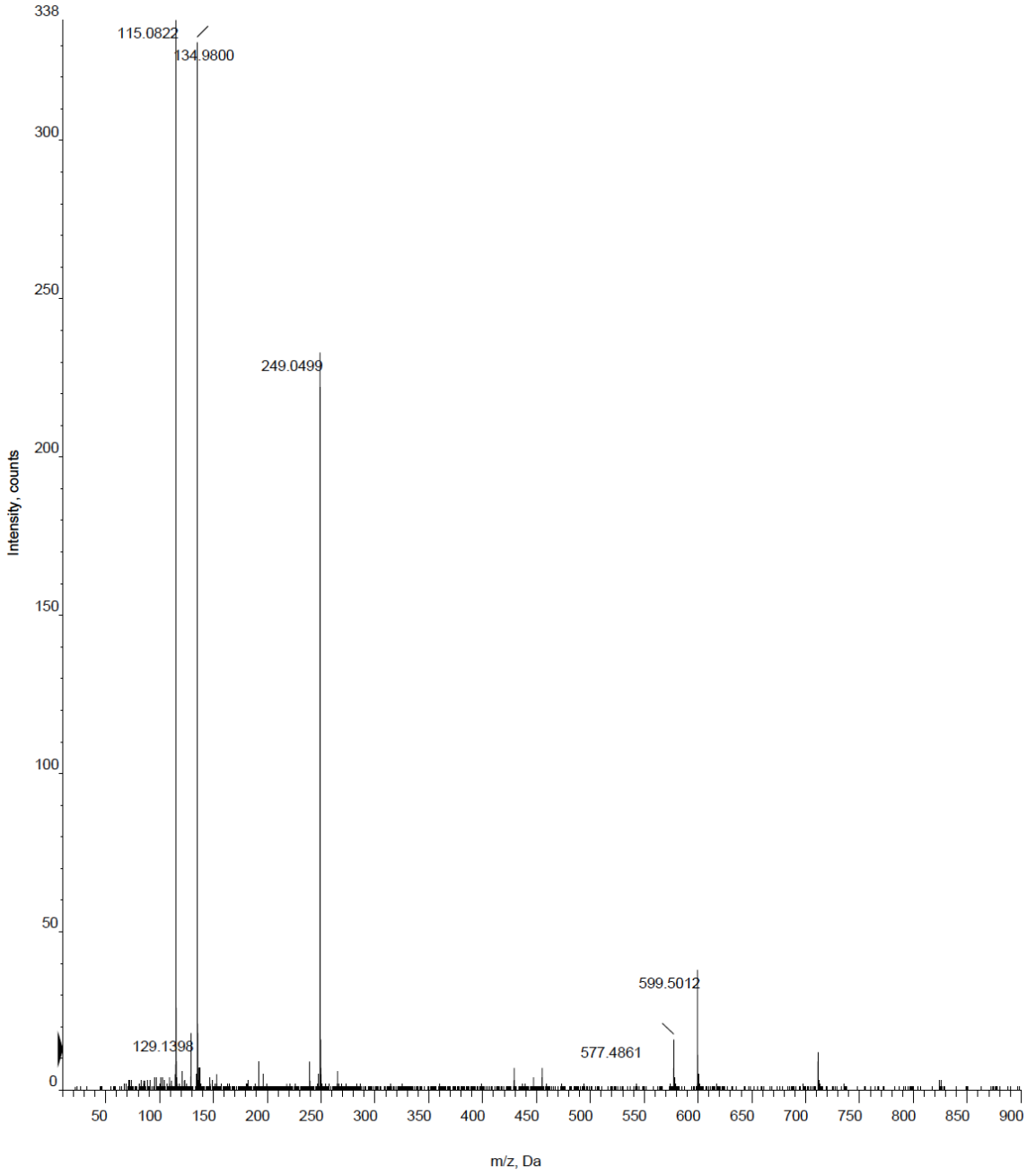

Figure 6.14: The product ion scan of the m/z 825.5 fragment ion.

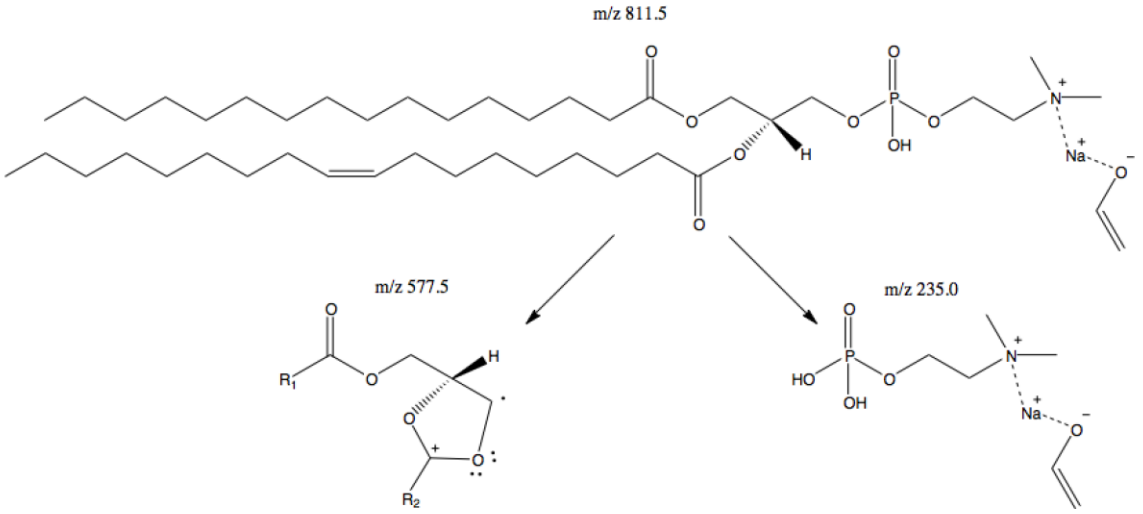

Figure 6.15: Fragmentation of the m/z 811.5 fragment ion.

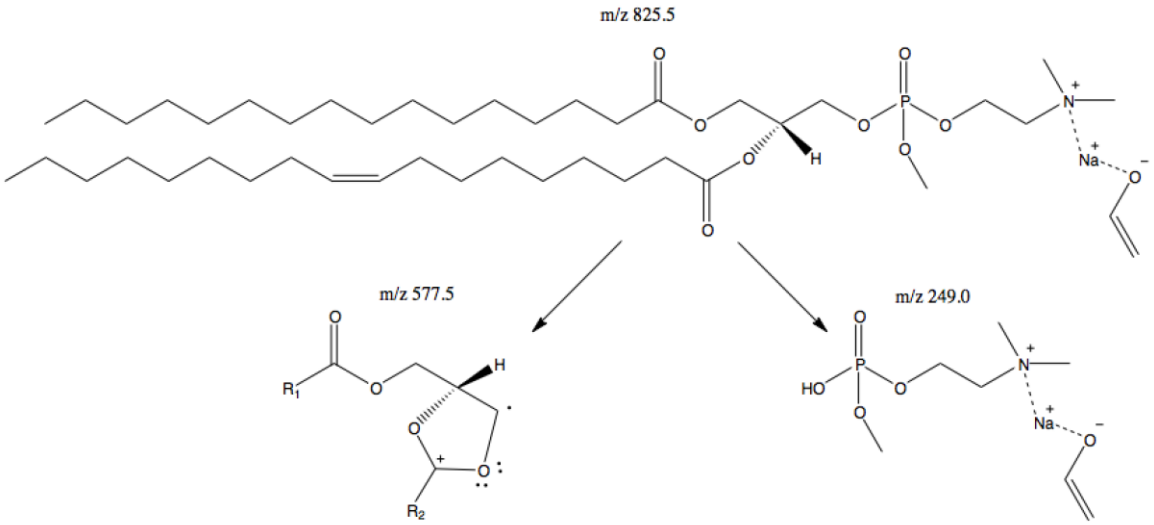

Figure 6.16: Fragmentation of the m/z 825.5 fragment ion.

6.2.2 Diazomethane reaction dynamics: sodium coordination inhibits SM methylation in methanol

A fresh 100 μM SM standard was prepared in MeOH. The SM peak splitting in the unmodified standard is attributed to protonated and sodiated species. The mass spectrum of this standard is shown in figure 6.18.

In a glass pipette vial, 50 μL of 100 μM SM in MeOH was methylated in 300 μL MeOH without HBF_4. The diazomethane vial consisted of 3 mL water, 225 mg *N*-Nitroso-*N*-methylurea, no ether, and 3 mL 8.9M KOH(aq). As shown in figure 6.19, this reaction produced once methylated SM with m/z 717.5, unmodified protonated SM with m/z 703.5 and unmodified sodiated SM with m/z 725.5. The methylation was 27% effective while the protonated peak accounted for 20% and the sodiated peak accounted for 53% of the unmodified product.

The same reaction mixture was used to do a second round of methylation. To this reaction mixture, 10 μL of 100 μM HBF_4 in MeOH and 100 μL of MeOH were added. The diazomethane vial consisted of 3 mL water, 228 mg *N*-Nitroso-*N*-methylurea, no ether, and 3 mL 8.9M KOH(aq). As shown in figure 6.20, this reaction produced once methylated SM with m/z 717.5 (38% peak intensity), unmodified protonated SM with m/z 703.5 (45% peak intensity) and unmodified sodiated SM with m/z 725.5 (17% peak intensity). Even though there was some conversion to the methylated product, the conversion was not complete. There was also a lot of remaining unmodified SM that was

protonated instead of sodiated compared to the previous reaction, which did not contain HBF_4.

The same reaction mixture from the second round of methylation sat in the freezer for four days. In that time, the unmodified lipid equilibrated with the acid, completely displacing the sodium. As a result, there was a methylated peak, unmodified protonated peak, and no sodiated peak. This mass spectrum is shown in figure 6.21.

The same reaction mixture underwent a third round of methylation with no additional acid. To this reaction mixture, only 100 μL of MeOH was added. The diazomethane vial consisted of 3 mL water, 205 mg *N*-Nitroso-*N*-methylurea, no ether, and 3 mL 8.9M KOH(aq). As shown in figure 6.22, this reaction produced once methylated SM with m/z 717.5 (48% peak intensity), unmodified protonated SM with m/z 703.5 (6% peak intensity), and unmodified sodiated SM with m/z 725.5 (46% peak intensity).

The fact that so much of the lipid was sodiated after the third round of methylation suggests that a significant amount of diazomethane was reacting with the solvent and the sodium could then coordinate with the lipid. In order for this to happen, the diazomethane would have to deprotonate the lipid's phosphate group, but then methylate the solvent.

The following day, the mass spectrum of this sample showed only protonated species and no sodiated species, indicating that it is thermodynamically favourable to protonate the phosphate group in an acidic solution. This demonstrates that the rate at which diazomethane acquires a proton and then methylates a substrate is faster than the rate at which the sodiated phosphate can exchange a proton. Not only is the rate of methylation faster, it is also non-specific. The fact that sodiated lipid is forming proves that the phosphate is deprotonated and not immediately methylated. This mass spectrum is shown in figure 6.23.

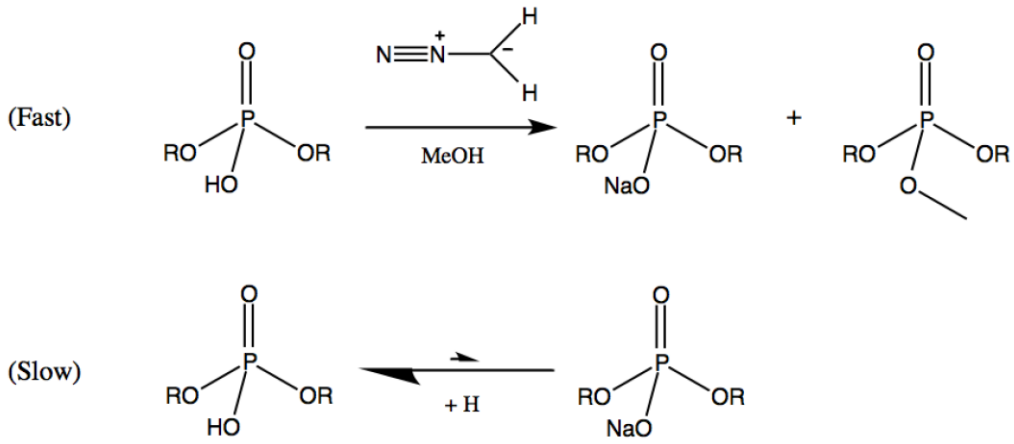

Figure 6.17: SM methylation kinetics in MeOH.

Immediately following the reaction, the mass spectrum shows it is kinetically favourable to form the sodiated species. This makes sense because as protons displace sodium in solution and MeOH is converted to dimethyl ether, the concentration of free sodium increases. Even though the sodiated species gradually reverts into the protonated species over time, the regeneration of the protonated species is not fast

enough in order to react with the diazomethane gas. As a result, when sodium coordinates with the phosphate group during the reaction, it inhibits methylation.

To accommodate the thermodynamics of this reaction, the flow rate of diazomethane was slowed down considerably with the intention to allow sodium displacement and promote more methylation. In a glass pipette vial, the reaction mixture consisted of 50 μL of 100 μM SM in MeOH, 200 μL MeOH, and 10 μL of 100 μM HBF_4 in MeOH. The lipid was allowed to equilibrate with the acid for 20 minutes prior to starting the reaction. To reduce the flow rate of diazomethane, 3 mL of a dilute KOH solution (325 mg in 5 mL water) was injected slowly over a 20-minute period through a 20G needle. As shown in figure 6.24, this reaction yielded protonated unmodified SM with m/z 703.5 and sodiated unmodified SM with m/z 725.5. The amount of methylated SM was negligible.

By reducing the flow rate of diazomethane over a period of 20 minutes, there was a considerable amount of time for the protons to displace sodium. This is evident in the mass spectrum, which shows the relative abundance of protonated and sodiated SM immediately following the reaction. Another conclusion that can be drawn from this experiment is that diazomethane does not methylate with specificity in MeOH. The fact that there was sodiated SM proves that the lipid was deprotonated and the negligible quantity of methylated SM suggests that the diazomethane mostly methylated the solvent.

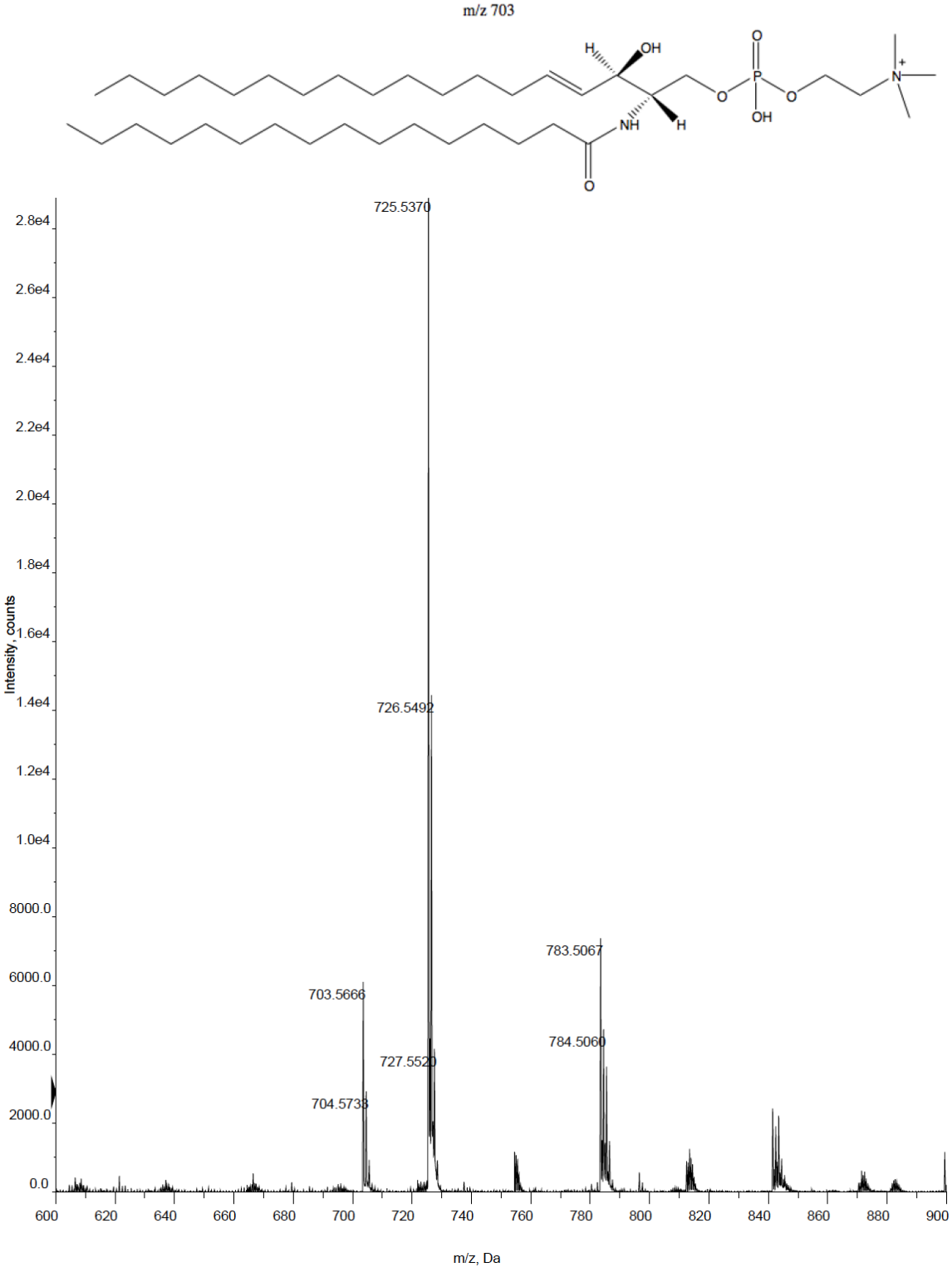

Figure 6.18: Unmodified 100μM SM standard in MeOH.

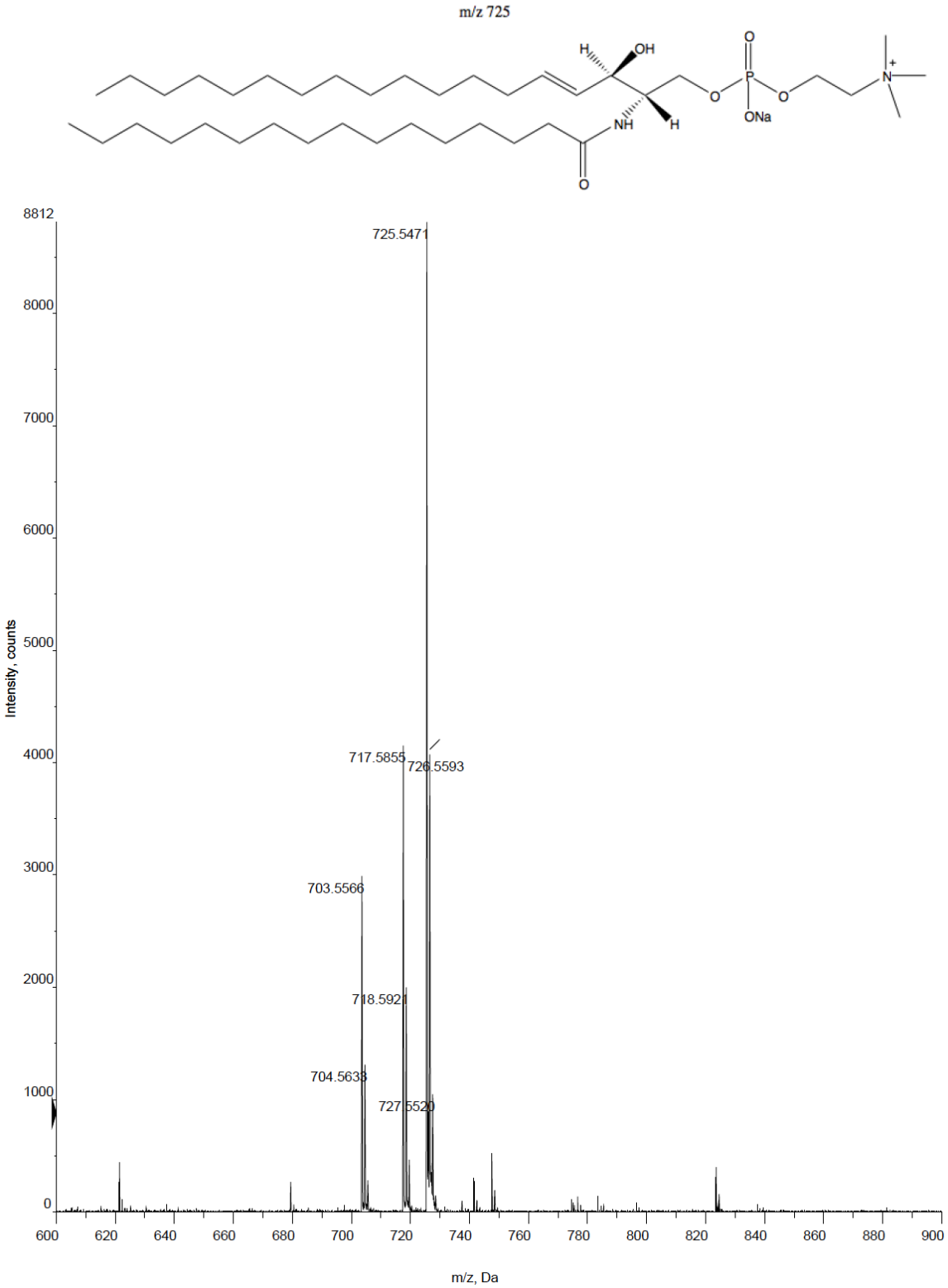

Figure 6.19: SM methylation after the first round of diazomethane without HBF_4.

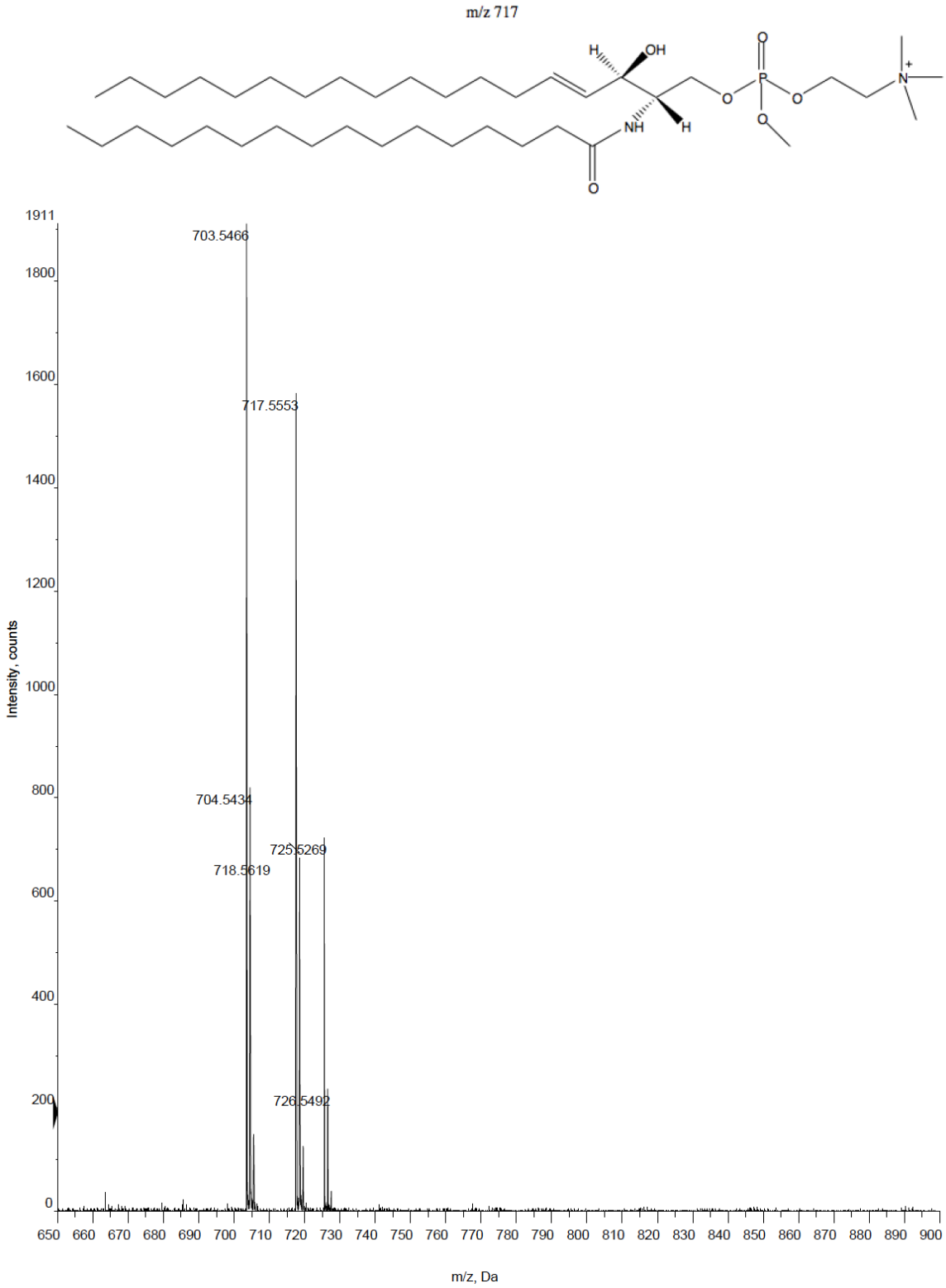

Figure 6.20: SM methylation after the second round of diazomethane with HBF_4.

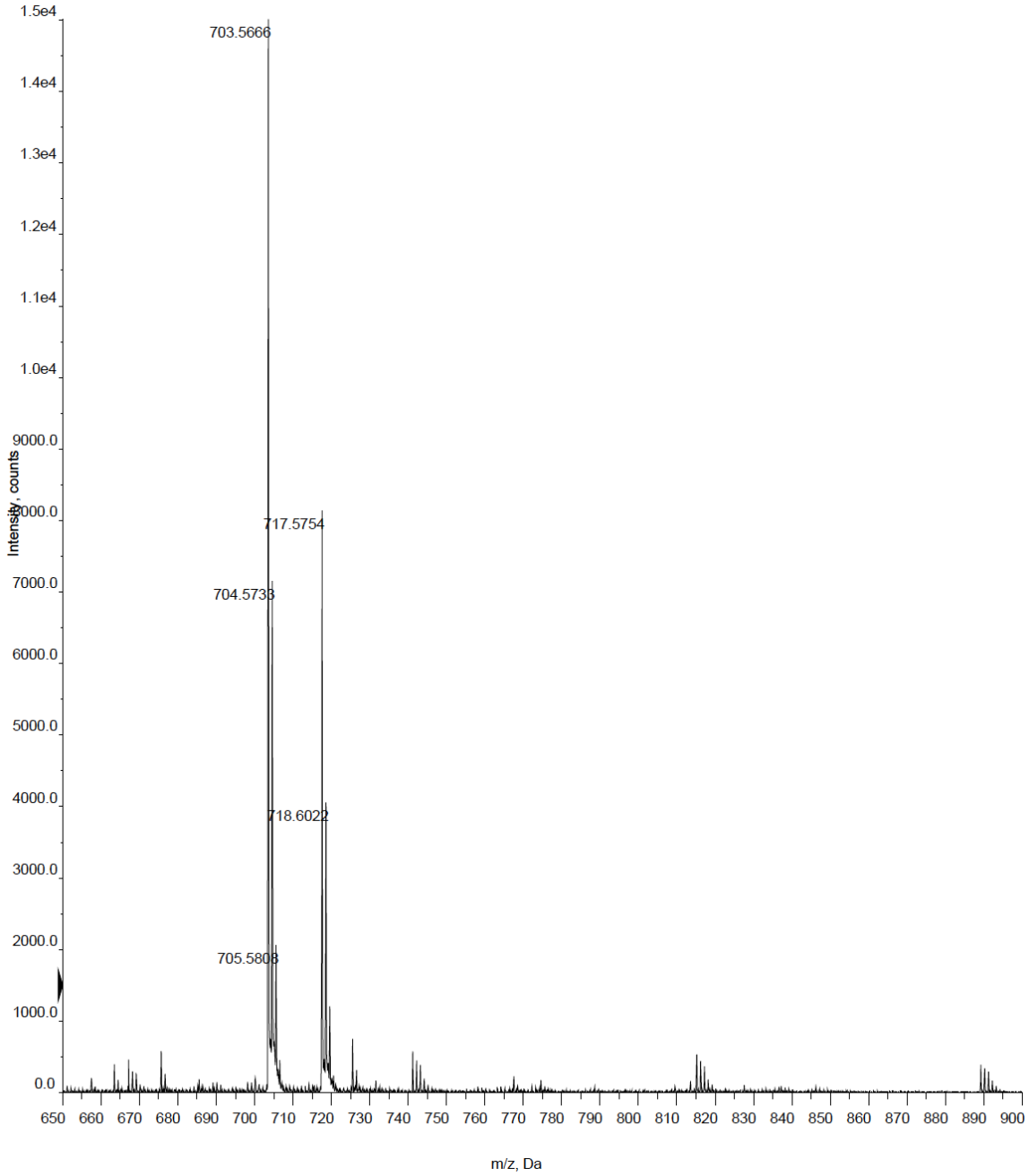

Figure 6.21: SM methylation after the second round of diazomethane with HBF_4. This sample was analyzed after equilibrating in a freezer for four days.

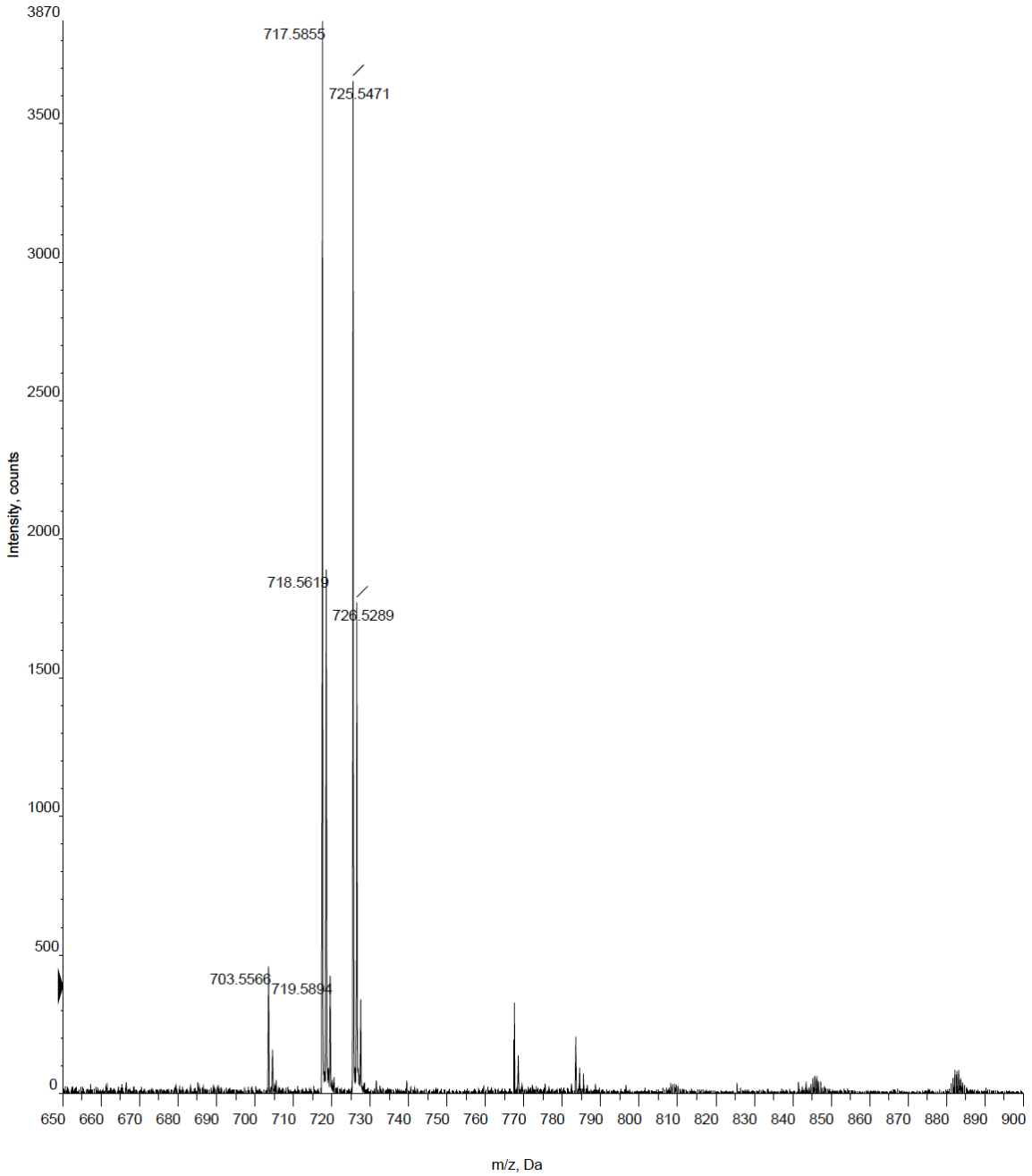

Figure 6.22: SM methylation after the third round of diazomethane. No additional HBF_4 was added after the second round.

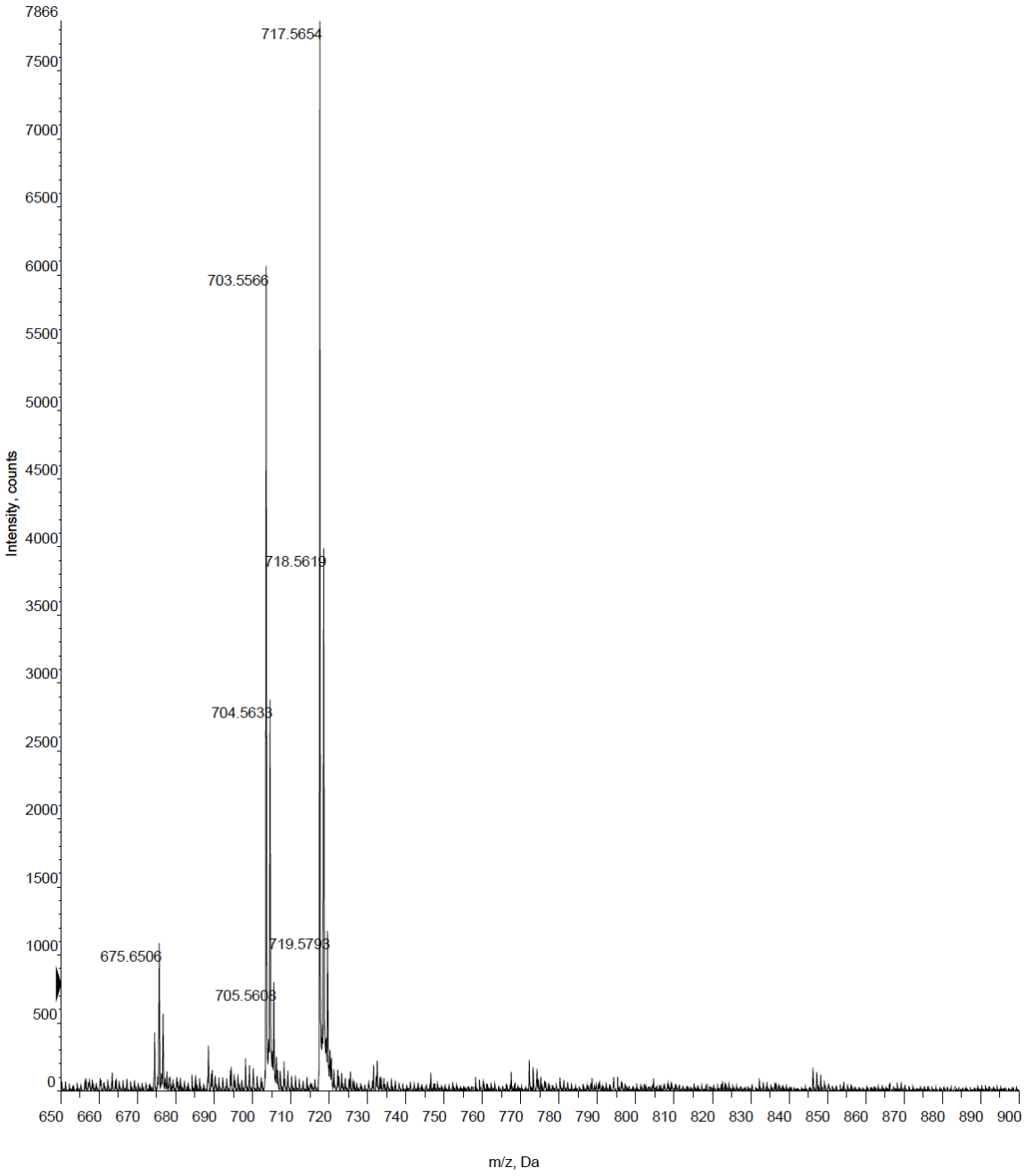

Figure 6.23: Third round of SM methylation without additional HBF_4 after the second round. This sample was analyzed after equilibrating in a freezer for 1 day.

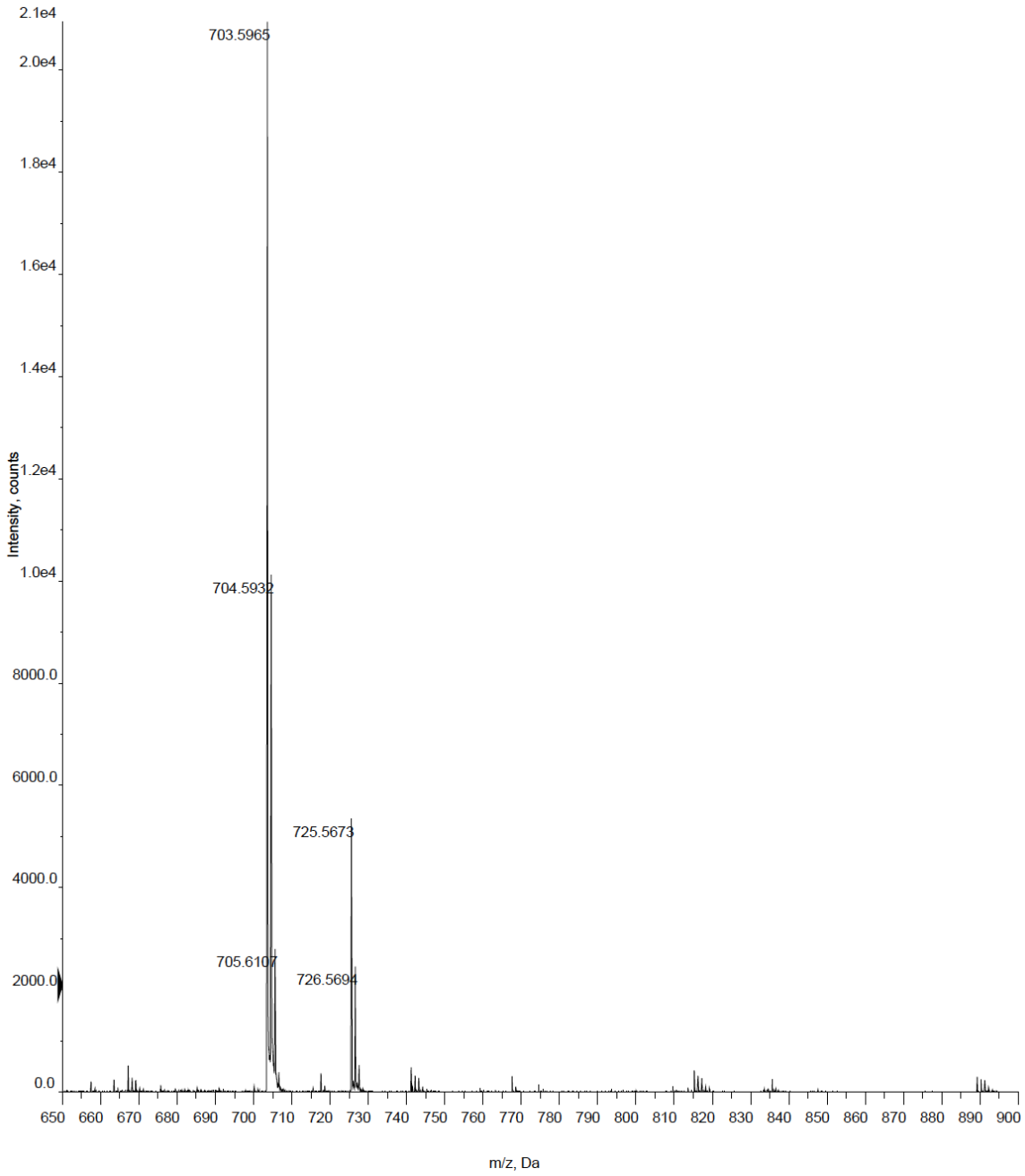

Figure 6.24: SM methylation resulting from reduced diazomethane flow rate.

6.2.3 Optimized signal in lipid standards

In a glass pipette vial, 50 μL of 100 μM PC in MeOH was methylated in roughly 300 μL ether and 5 μL of 100 μM HBF_4 in MeOH. The diazomethane vial consisted of 3 mL water, 216 mg *N*-Nitroso-*N*-methylurea, and 3 mL 8.9M KOH(aq). A 100 μL aliquot of MeOH was added to the reaction mixture once the reaction was complete. This reaction produced once methylated PC with m/z 774.5. The mass spectrum of this sample is shown in figure 6.25.

In a glass pipette vial, 50 μL of 100 μM SM in EtOH was methylated in roughly 200 μL ether, 100 μL EtOH, and 10 μL of 100 μM HBF_4 in EtOH. The diazomethane vial consisted of 2 mL water, 212 mg *N*-Nitroso-*N*-methylurea, and 3 mL 8.9M KOH(aq). This reaction produced once methylated SM with m/z 717.5. The mass spectrum of this sample is shown in figure 6.26.

In a glass pipette vial, 50 μL of 100 μM PE in MeOH was dried down and methylated in roughly 300 μL ether, and 10 μL of 100 μM HBF_4 in MeOH. The diazomethane vial consisted of 2 mL water, 211 mg *N*-Nitroso-*N*-methylurea, and 3 mL 8.9M KOH(aq). A 100 μL aliquot of MeOH was added to the reaction mixture once the reaction was complete. This reaction produced four times methylated PE with m/z 774.5. The mass spectrum of this sample is shown in figure 6.27.

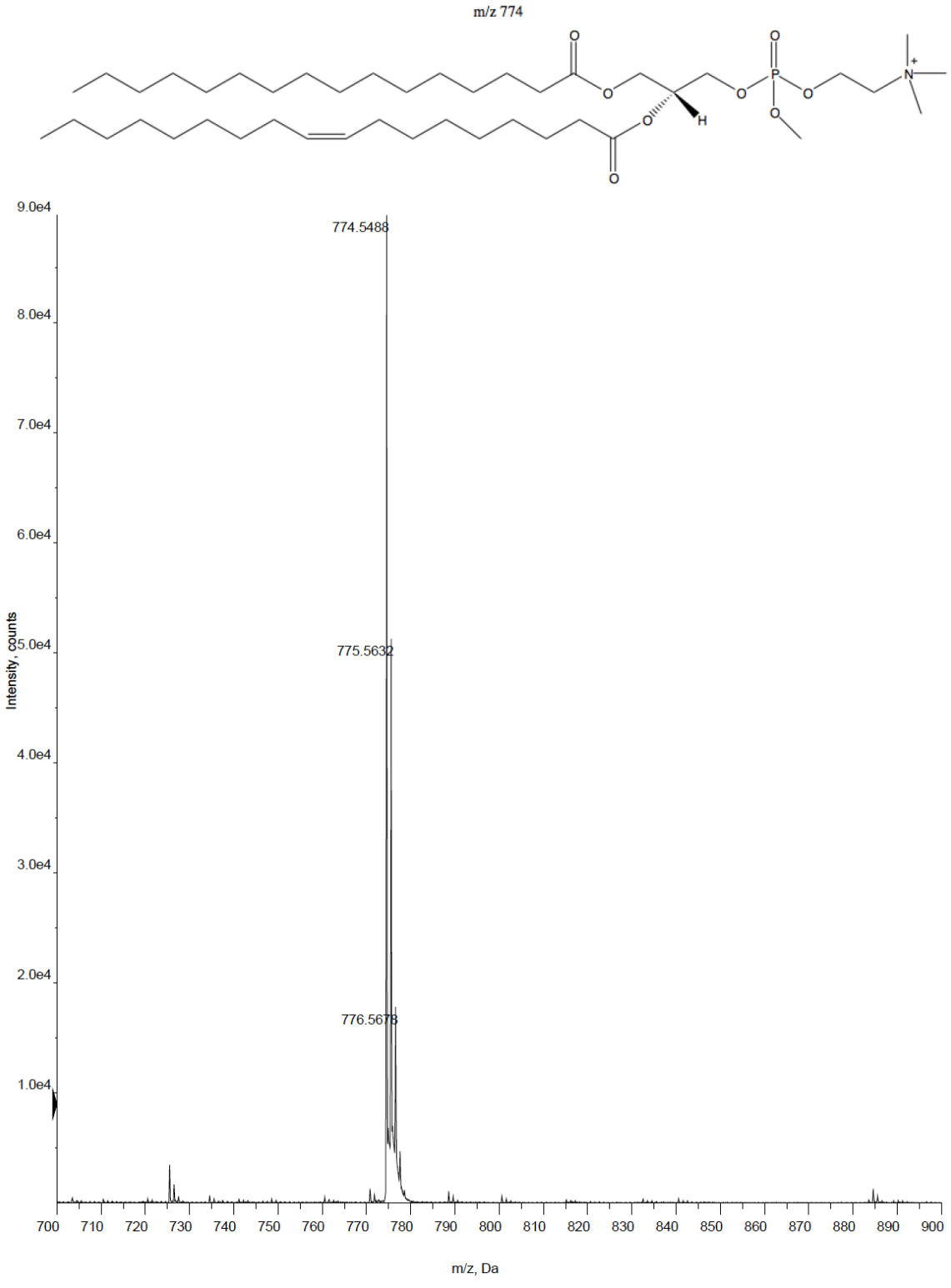

Figure 6.25: Optimized PC methylation in 75% ether and 25% MeOH.

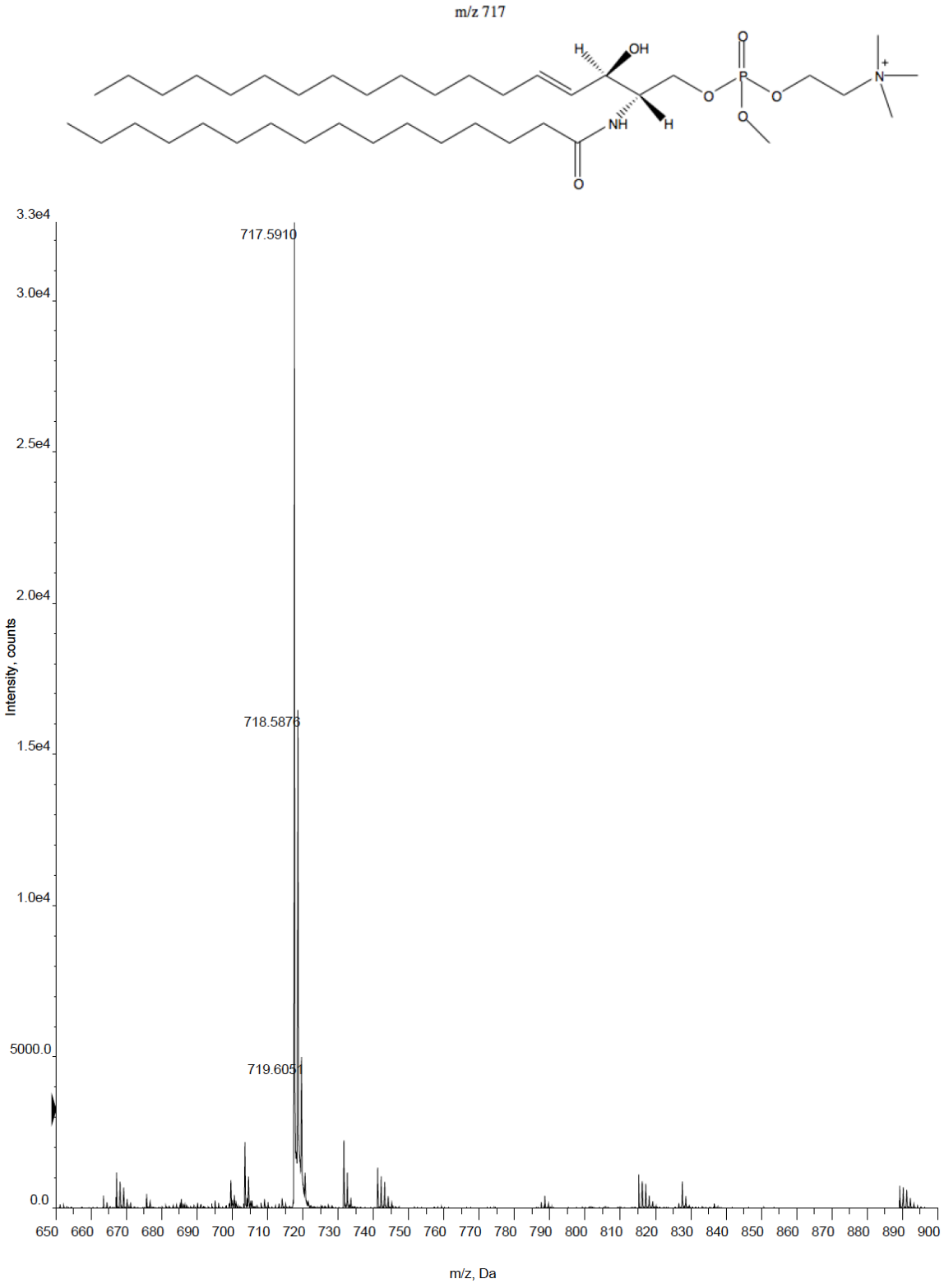

Figure 6.26: Optimized SM methylation in 50% ether and 50% EtOH.

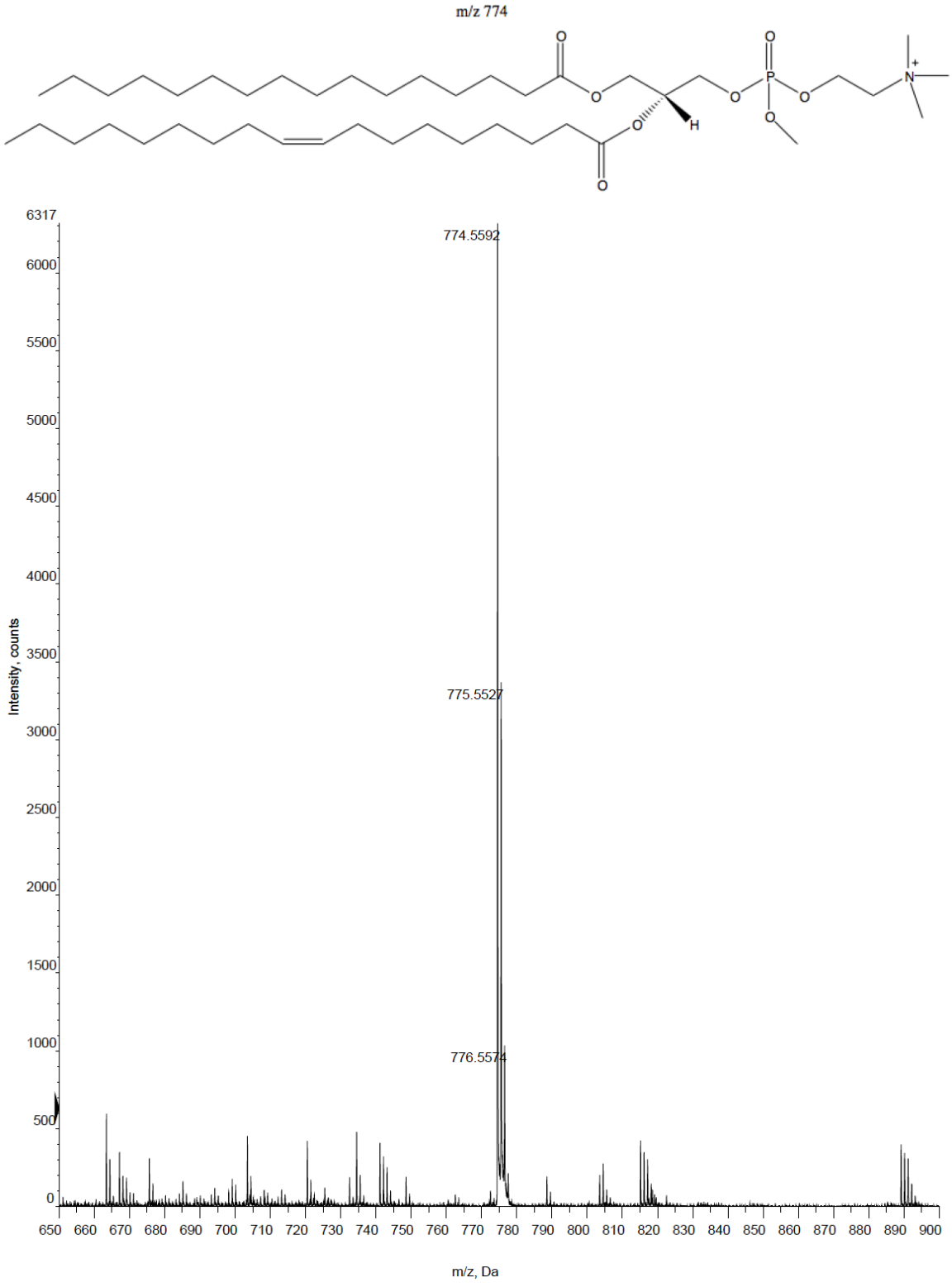

Figure 6.27: Optimized PE four times methylated in 100% ether.

6.2.4 SM methylation reaction solvent efficiency

The SM methylation reaction conditions were set for methylating 50 μL of 100 μM SM in MeOH or EtOH. For each reaction, the diazomethane vial consisted of 2 mL water, approximately 212 mg N-Nitroso-N-methylurea, and 3 mL 8.9M KOH(aq).

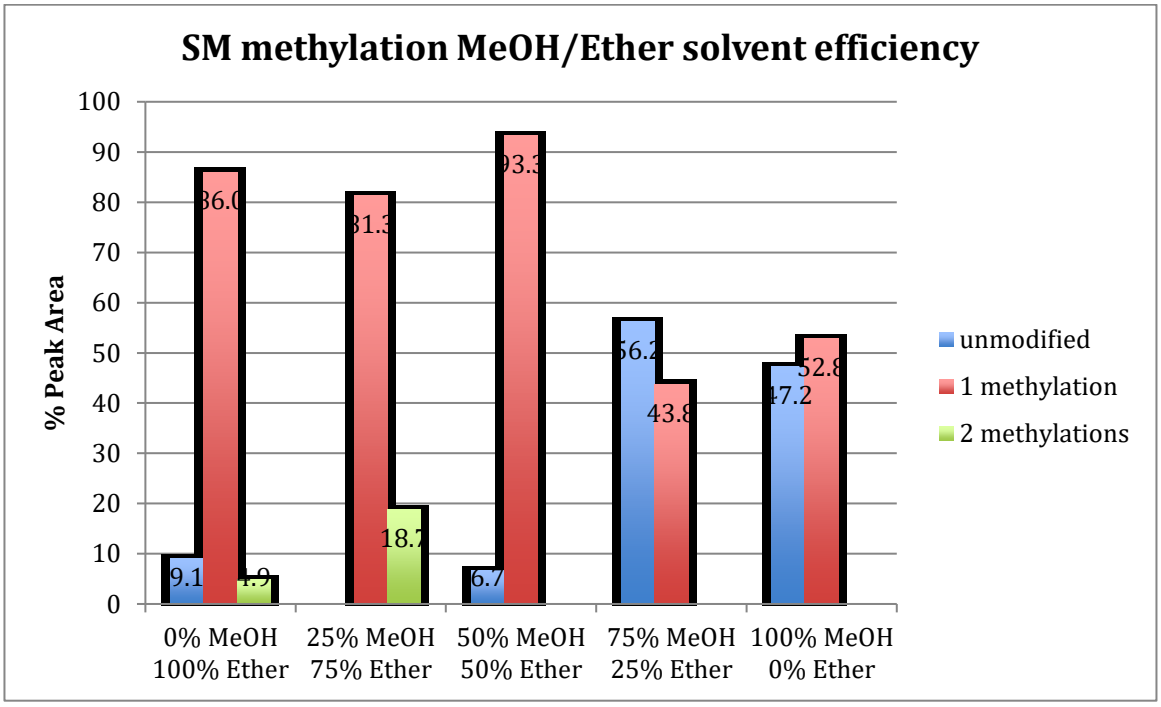

Figure 6.28: Distribution of products as a result of methylating SM in various mixtures of MeOH and ether.

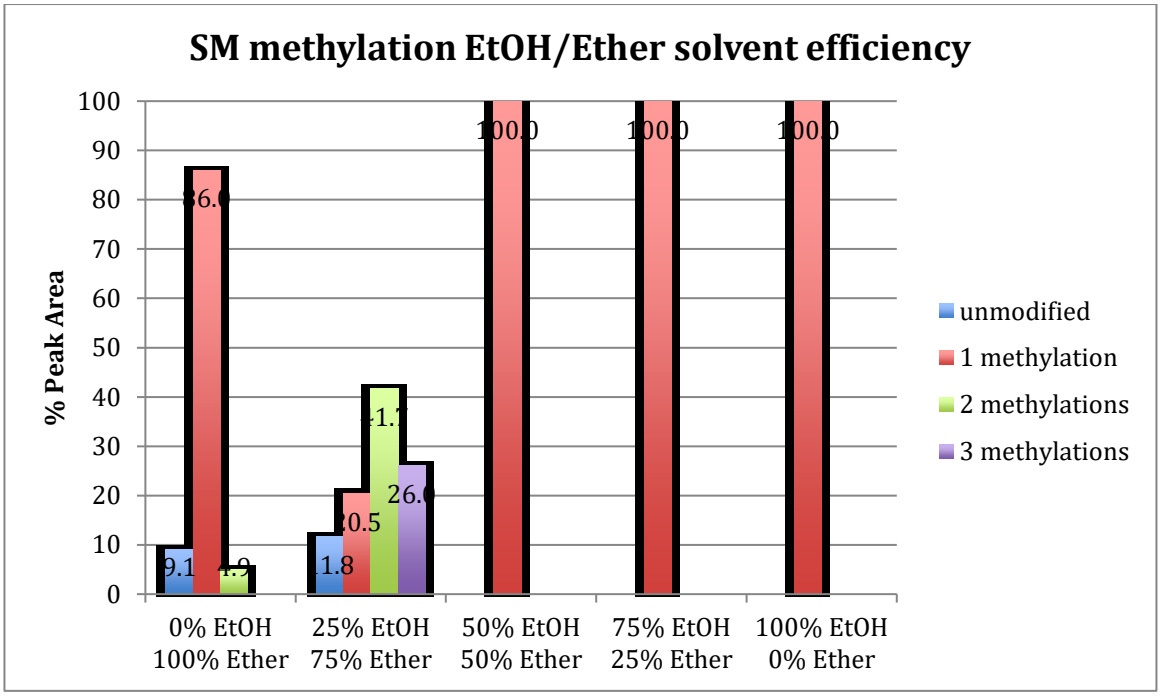

Figure 6.29: Distribution of products as a result of methylating SM in various mixtures of EtOH and ether.

The difference between using MeOH and using EtOH for methylating SM becomes apparent in this dataset. None of the MeOH/ether solvent mixtures achieved complete conversion to a once methylated SM species. However, complete conversion was achieved using EtOH in a range of 50-100% by volume.

In order to effectively methylate SM at the phosphate position using diazomethane, the phosphate anion must not compete with other stronger nucleophiles. During the reaction, once diazomethane is protonated, a nearby nucleophile can attack the electrophilic methyl carbon. This means that a protic solvent could potentially act as

a competitive nucleophile, the outcome of which is made apparent in this dataset. While neglecting to address subtle differences in the solvent mixtures, the nucleophilicity of EtOH is significantly less than MeOH, which is why SM is completely converted to the once methylated product in 50%, 75%, and 100% EtOH when mixed with ether. The obvious consequence of nucleophile competition is producing more unmodified SM.

In addressing the subtle details of the reaction, too much ether results in multiple methylations. Since the diazomethane mechanism involves proton exchange, a protic solvent to some extent helps regulate proton exchange. When using mostly ether, an aprotic solvent, SM must interact with diazomethane in a medium starved of protons, causing methylation to take place at less acidic moieties including the hydroxyl and the amide positions.

Table 6.1: Methylation of SM in varying solvent mixtures consisting of MeOH and ether.

Solvent Mix	100 μM SM	100 μM HBF_4	Ether	MeOH
0% MeOH 100% Ether	50 μL dried down	5 μL in MeOH	300 μL	0 μL
25% MeOH 75% Ether	50 μL in MeOH	10 μL in MeOH	250 μL	0 μL
50% MeOH 50% Ether	50 μL in MeOH	5 μL in MeOH	150 μL	100 μL
75% MeOH 25% Ether	50 μL in MeOH	5 μL in MeOH	100 μL	200 μL
100% MeOH 0% Ether	50 μL in MeOH	5 μL in MeOH	0 μL	200 μL

Table 6.2: Methylation of SM in varying solvent mixtures consisting of EtOH and ether.

Solvent Mix	100 μM SM	100 μM HBF_4	Ether	EtOH
0% EtOH 100% Ether	50 μL dried down	5 μL in EtOH	300 μL	0 μL
25% EtOH 75% Ether	50 μL in EtOH	5 μL in EtOH	250 μL	0 μL
50% EtOH 50% Ether	50 μL in EtOH	10 μL in EtOH	150 μL	100 μL
75% EtOH 25% Ether	50 μL in EtOH	5 μL in EtOH	100 μL	200 μL
100% EtOH 0% Ether	50 μL in EtOH	5 μL in EtOH	0 μL	200 μL

6.2.5 PE methylation reaction solvent efficiency

The PE methylation reaction conditions were set for methylating 50 μL of 100 μM PE in MeOH or EtOH. For each reaction, the diazomethane vial consisted of 2 mL water, approximately 212 mg *N*-Nitroso-*N*-methylurea, and 3 mL 8.9M KOH(aq).

Ether is the most effective solvent for completely methylating PE (one methylation at the phosphate and three methylations on the amine). Since ether is aprotic, the only acidic protons available with which diazomethane can react are at the phosphate and amine sites on PE. Ether also efficiently solvates diazomethane, keeping it dissolved and preventing it from passing through the solution unreacted. As a result, ether increases the reactivity and selectivity of diazomethane towards the polar head group region of PE.

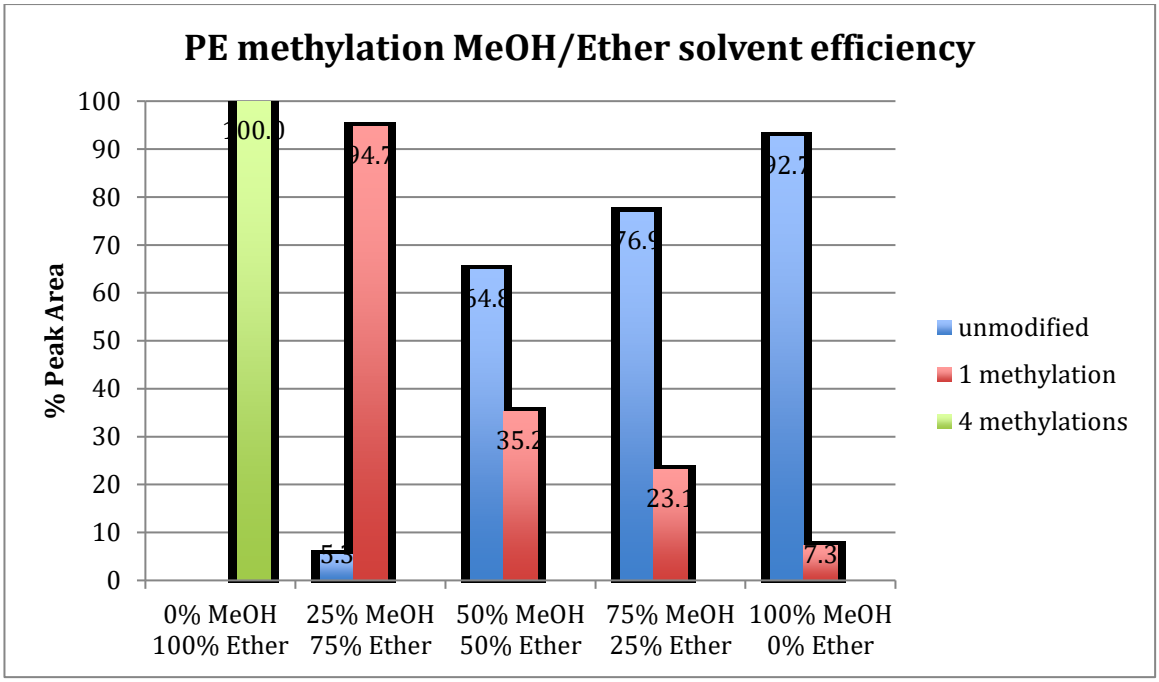

Figure 6.30: Distribution of products as a result of methylating PE in various mixtures of MeOH and ether.

MeOH is a protic solvent, and so it will react with diazomethane. MeOH acts as a nucleophile in competition with the phosphate and amine groups. As a result, more MeOH causes decreased methylation. One thing to note is the lack of twice or thrice methylated PE. This is likely due to MeOH being more acidic than the amine protons, which would mean that MeOH only competes with the phosphate group for methylation. In that case, it would be possible that twice or thrice methylated PE could form in a solvent mixture with less than 25% MeOH.

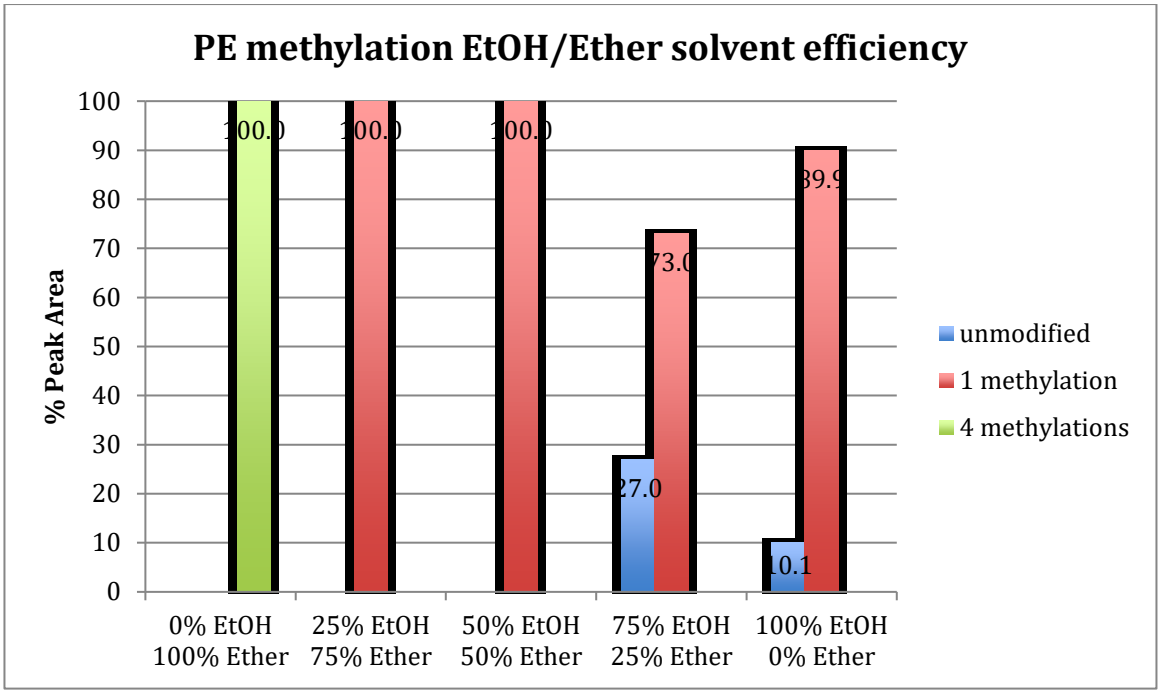

Figure 6.31: Distribution of products as a result of methylating PE in various mixtures of EtOH and ether.

EtOH is a protic solvent, but acts as a relatively poor nucleophile with respect to phosphate, which means that methylation is more selective towards the phosphate position. EtOH is also more acidic than the amine protons, which caps the reaction at one methylation, since deprotonating the amine is unfavourable. As a result, PE is completely converted to being methylated at the phosphate position when the solvent ranges from 25% to 50% EtOH in ether. The ether increases the reactivity of the diazomethane by solvating it, without consuming it. At higher levels of EtOH, more diazomethane is consumed by the solvent instead of reacting with PE, resulting in a mixture of once methylated and unmodified PE.

Table 6.3: Methylation of PE in varying solvent mixtures consisting of MeOH and ether.

Solvent Mix	100 μM PE	100 μM HBF_4	Ether	MeOH
0% MeOH 100% Ether	50 μL dried down	10 μL in MeOH	300 μL	0 μL
25% MeOH 75% Ether	50 μL in MeOH	10 μL in MeOH	250 μL	0 μL
50% MeOH 50% Ether	50 μL in MeOH	10 μL in MeOH	150 μL	100 μL
75% MeOH 25% Ether	50 μL in MeOH	10 μL in MeOH	100 μL	200 μL
100% MeOH 0% Ether	50 μL in MeOH	10 μL in MeOH	0 μL	200 μL

Table 6.4: Methylation of PE in varying solvent mixtures consisting of EtOH and ether.

Solvent Mix	100 μM PE	100 μM HBF_4	Ether	EtOH
0% EtOH 100% Ether	50 μL dried down	10 μL in EtOH	300 μL	0 μL
25% EtOH 75% Ether	50 μL in EtOH	10 μL in EtOH	250 μL	0 μL
50% EtOH 50% Ether	50 μL in EtOH	10 μL in EtOH	150 μL	100 μL
75% EtOH 25% Ether	50 μL in EtOH	10 μL in EtOH	100 μL	200 μL
100% EtOH 0% Ether	50 μL in EtOH	10 μL in EtOH	0 μL	200 μL

6.3 Conclusion

In attempting to methylate PE in EtOH under non-acidic conditions, an unusual complex formed. The mass spectral data supports the formation of a PE enolate complex with sodium, which suggests that diazomethane acted as a strong base.

In attempting to methylate SM in MeOH under acidic conditions, the efficiency of the methylation was not in agreement with the believed mechanism of diazomethane. As a result, the reaction was probed and showed that diazomethane does not methylate SM with specificity in MeOH and that sodium inhibits SM methylation.

SM and PE were methylated in varying amounts of MeOH or EtOH with ether to find optimal solvent mixtures. SM was completely converted to the once methylated product in mixtures consisting of 50:50, 75:25, and 100:0 ratios of EtOH/ether. PE was completely converted to the four times methylated product in ether. PE was also completely converted to the once methylated product in mixtures consisting of 25:75 and 50:50 ratios of EtOH/ether.

6.4 Future works

The mechanism by which diazomethane operates in various solvent mixtures is now better understood. Moving forward, one major obstacle is that SM and PE have poor overlap in terms of their optimal solvent conditions for complete methylation. In order to accurately quantify these phospholipids from biological samples, there would likely need to be a lipid extraction step followed by two separate methylation reactions. Having two methylation reactions would accommodate the optimal solvent conditions for SM and PE. Using these solvent conditions, methylated standards of each phospholipid can be prepared in various concentrations to form a calibration curve for quantification. Fortunately, PC can be completely methylated in several solvent mixtures and so its quantification can be obtained in addition to SM and PE without any extra hassle.

6.5 References

18. Crowther, J. G. British Scientists of the Twentieth Century 9; Routledge: New York, USA, 2009; pp 15-21.

19. Griffiths, I. W.; *Rapid Communications In Mass Spectrometry*. **1997**, *11*, pp 7-14.

20. Gross, J. H. *Mass Spectrometry*, 2nd ed.; Springer-Verlag: Heidelberg, 2011; pp 123.

21. Vance, J. E. *Journal of Lipid Research*. **2008**, *49*, 1377-1387.

22. Noga, A. A.; Vance, D. E. *Journal of Lipid Research*. **2003**, *44*, 1998-2005.

23. Yamazaki, K.; Masaki, N.; Kohmura-Kobayashi, Y.; Yaguchi, C.; Hayasaka, T.; Itoh, H.; Setou, M.; Kanayama, N. *Phospholipid Molecular Species and Placental Pathology*. **2015**, PLoS ONE 10(11): e0142609.

24. Wasslen, K. V.; Tan, L. H.; Manthorpe, J. M.; Smith, J. C. *Anal. Chem.* **2014**, *86*, 3291-3299.

25. Canez, C. R.; Shields, S. W. J.; Bugno, M.; Wasslen, K. V.; Weinert, H. P.; Willmore, W. G.; Manthorpe, J. M.; Smith, J. C. *Anal. Chem.* **2016**, *88*, 6996-7004.

26. Arndt, F., Diazomethane, *Org. Synth.* **1935**, *15*, 3.

27. Arndt, F., Nitrosomethylurea. *Org. Synth*. **1943**, *2*, 461.

28. Golding, B. T.; Bleasdale, C.; McGinnis, J.; Müller, S.; Rees, H. T.; Rees, N. H.; Farmer, P. B.; Watson, W. P. *Tetrahedron.* **1997**, *53:11*, pp. 4065.